Measurement of the weak neutral form-factor of the proton at high momentum transfer

Kent Paschke
University of Virginia

E12-23-004

Spokespeople: R.Beminiwattha, D.Hamilton, C. Palatchi, KP, **B.Wojtsekhowski**

LaTech, Glascow, Indiana, UVa, JLab, CUA, INFN - Roma, Temple, Ohio, Syracuse, FIU, CNU, Fermilab, UWashington, Tel Aviv U, Hebrew U, W&M, AANL Yerevan, Northern Michigan, UConn, Orsay

Nucleon Form Factors at High Q^2

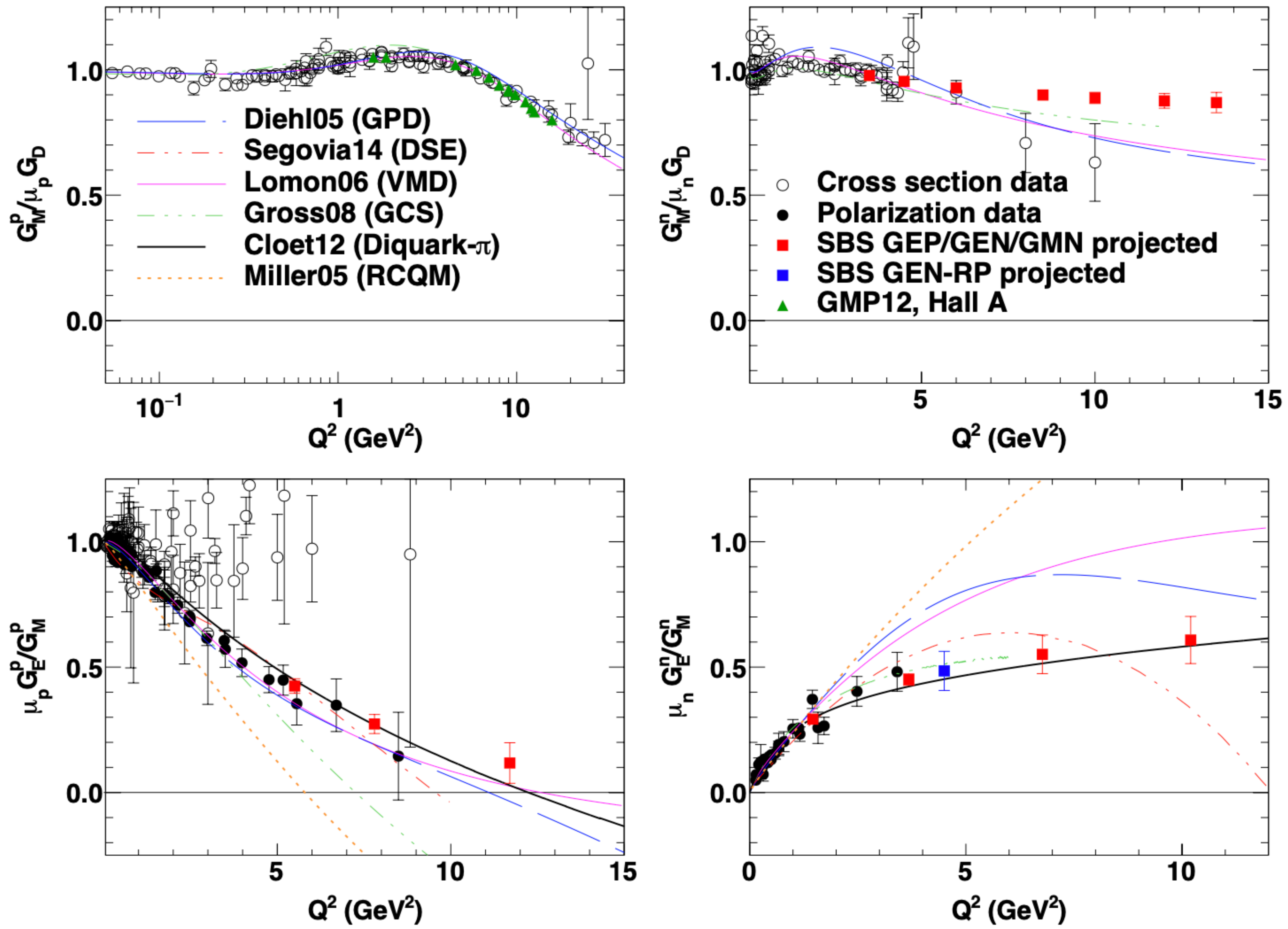

Prog.Part.Nucl.Phys. 127 (2022) 103985

- One might expect a transition to perturbatively dominated mechanisms
- Other degrees of freedom might become evident, such as orbital angular momentum or diquark structure
- Part of the 3D mapping of nucleon structure as the first moment of GPDs at $\xi = 0$

$$\int_{-1}^{+1} dx\, H^q(x,0,Q^2) = F_1^q(Q^2)$$

$$\int_{-1}^{+1} dx\, E^q(x,0,Q^2) = F_2^q(Q^2)$$

These implications rely on extracting the independent quark contributions

Flavor Separation of Nucleon Form Factors

These implications rely on extracting the independent quark contributions

$$F^u_{1(2)} = 2\,F^p_{1(2)} + F^n_{1(2)} \quad \text{and} \quad F^d_{1(2)} = 2\,F^n_{1(2)} + F^p_{1(2)}$$

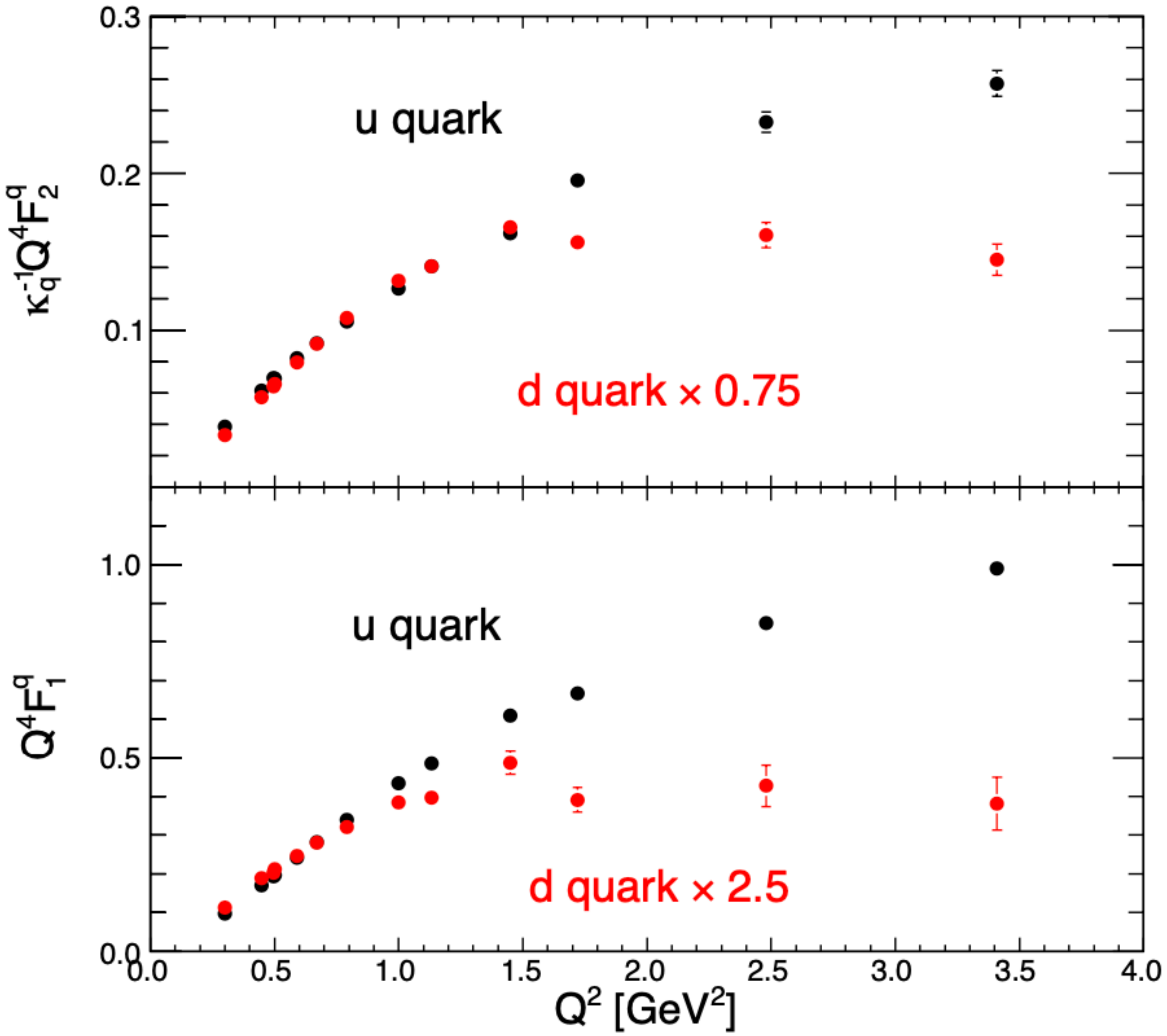

G. Cates et al. Phys. Rev Lett. 106 (2011)

For example: the apparent onset of Q^4 scaling for d-quark form-factors has been suggested to be consistent with the emergence of perturbative behavior in scattering and with the minority quark tied up in a diquark structure

This is speculative, but there is a strong effort to extend this data to higher Q^2

Charge symmetry and the nucleon form factors

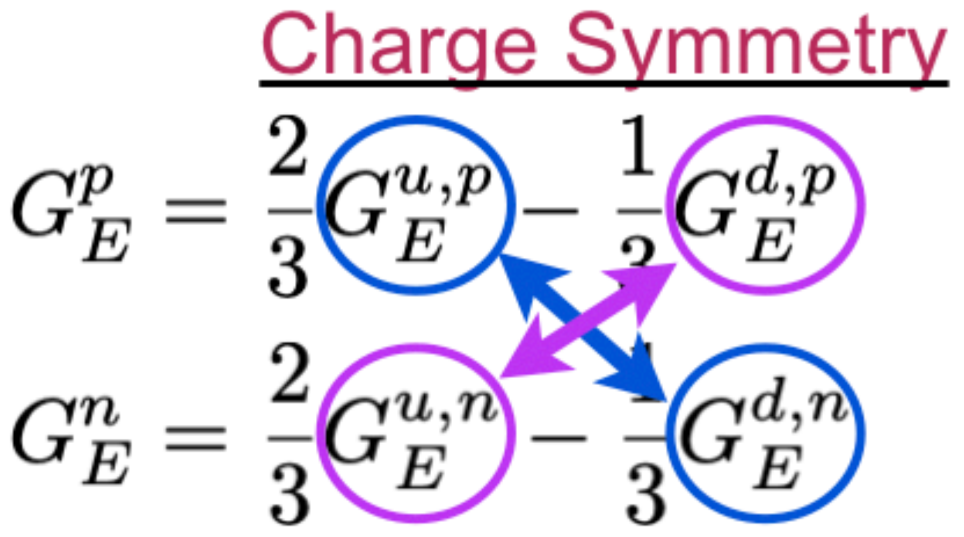

Charge symmetry is assumed for the form factors, $G_E^{u,p} = G_E^{d,n}$, *etc.* and used to find the flavor separated form-factors, measuring $G_{E,M}^{p,n}$ to find $G_{E,M}^{u,d}$

$$G_E^p = \frac{2}{3}G_E^{u,p} - \frac{1}{3}G_E^{d,p} - \frac{1}{3}G_E^s$$
$$G_E^n = \frac{2}{3}G_E^{u,n} - \frac{1}{3}G_E^{d,n} - \frac{1}{3}G_E^s$$

But this can broken! One way is to have a non-zero strange form-factor, which breaks the "2 equations and 2 unknowns" system

The weak form factor provides a third linear combination:

$$G_E^{p,Z} = \left(1 - \frac{8}{3}\sin^2\theta_W\right)G_E^{u,p} + \left(-1 + \frac{4}{3}\sin^2\theta_W\right)G_E^{d,p} + \left(-1 + \frac{4}{3}\sin^2\theta_W\right)G_E^s$$

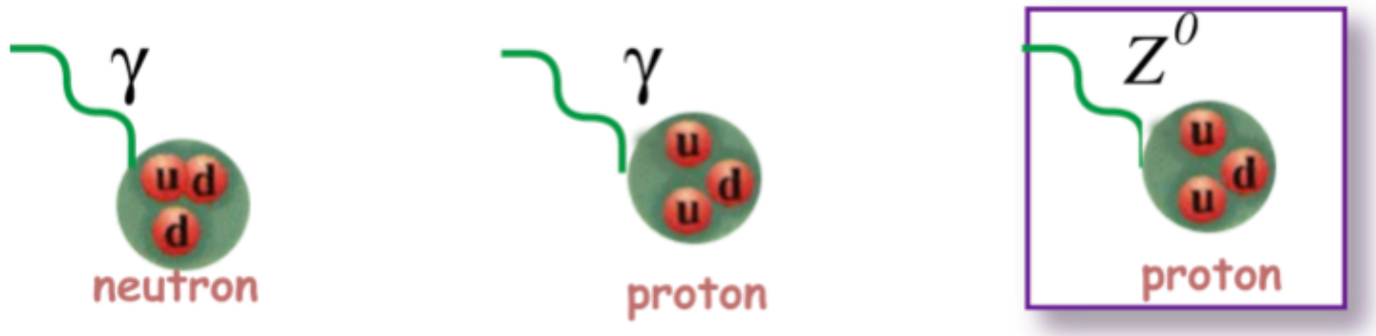

A strange quark form factor would be indistinguishable from a broken charge symmetry in u,d flavors

$$\delta G_E^u \equiv G_E^{u,p} - G_E^{d,n}$$
$$\delta G_E^d \equiv G_E^{d,p} - G_E^{u,n}$$

So, more generally: the assumption of charge symmetry is crucial to the flavor decomposition of the form factors

Parity Violating Electron Scattering

Elastic e-p scattering with longitudinally polarized beam and unpolarized target:

Weak and EM amplitudes interfere:

$$\sigma = |\mathcal{M}_\gamma + \mathcal{M}_Z|^2$$

$$A_{PV} = \frac{\sigma_R - \sigma_L}{\sigma_R + \sigma_L} \sim$$

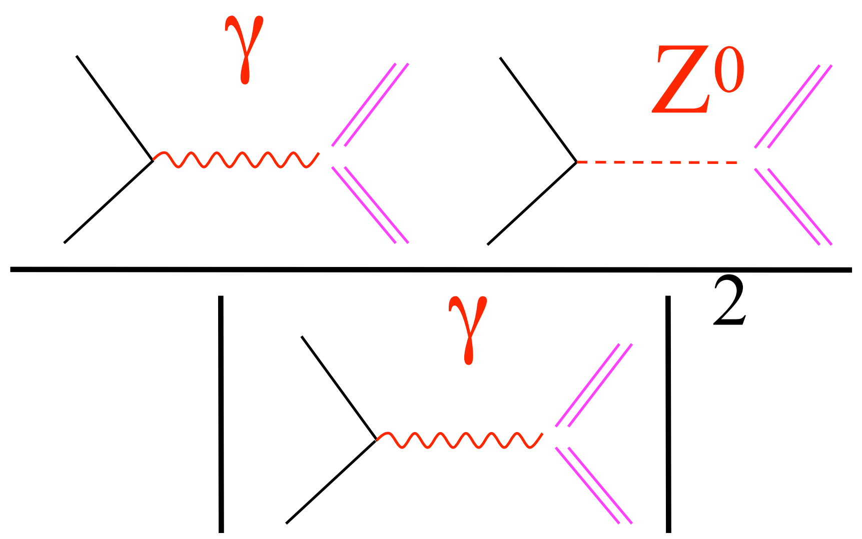

$$\approx \frac{|\mathcal{M}_Z|}{|\mathcal{M}_\gamma|}$$

Expressing A_{PV} for e-p scattering, with proton and neutron EM form-factors plus strange form factors:

$$A_{PV} = -\frac{G_F Q^2}{4\pi\alpha\sqrt{2}} \cdot [(1-4\sin^2\theta_W) - \frac{\epsilon G_E^p G_E^n + \tau G_M^p G_M^n}{\epsilon (G_E^p)^2 + \tau (G_M^p)^2} - \frac{\epsilon G_E^p G_E^s + \tau G_M^p G_M^s}{\epsilon (G_E^p)^2 + \tau (G_M^p)^2}$$
$$+ \epsilon'(1-4\sin^2\theta_W)\frac{G_M^p G_A^{Zp}}{\epsilon (G_E^p)^2 + \tau (G_M^p)^2}]$$

This technique was used to hunt for indications of strange quark contributions in the nucleon, particularly in the *static* (*i.e.* $Q^2 \rightarrow 0$) properties: a strange charge radius or strange magnetic moment

Proton strange form factors via parity violating elastic electron scattering

Strange form factors are measured to be consistent with zero at low Q^2,
but do not rule out non-zero values at higher Q^2,
especially for magnetic form factor which is more accessible at higher Q^2

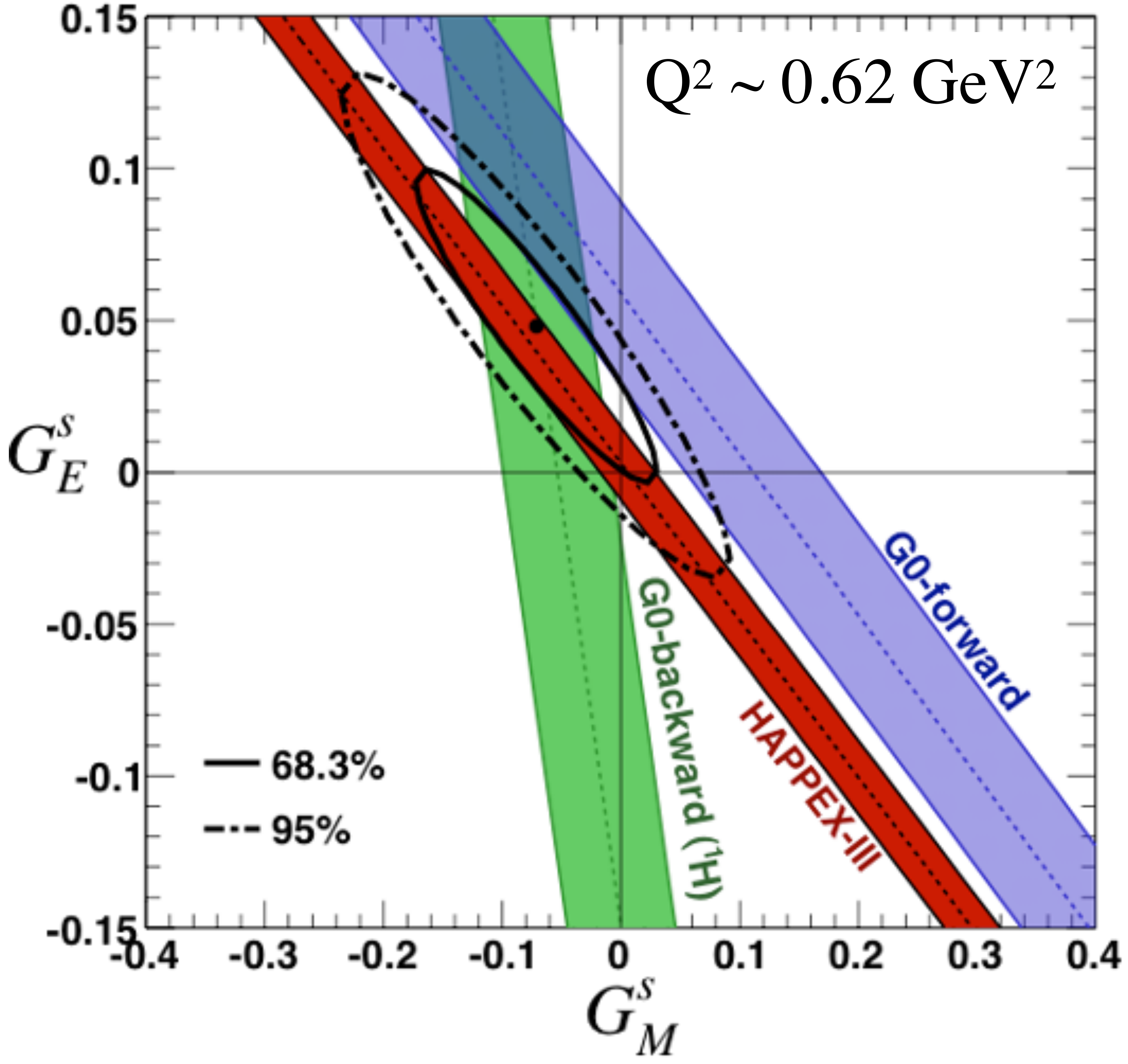

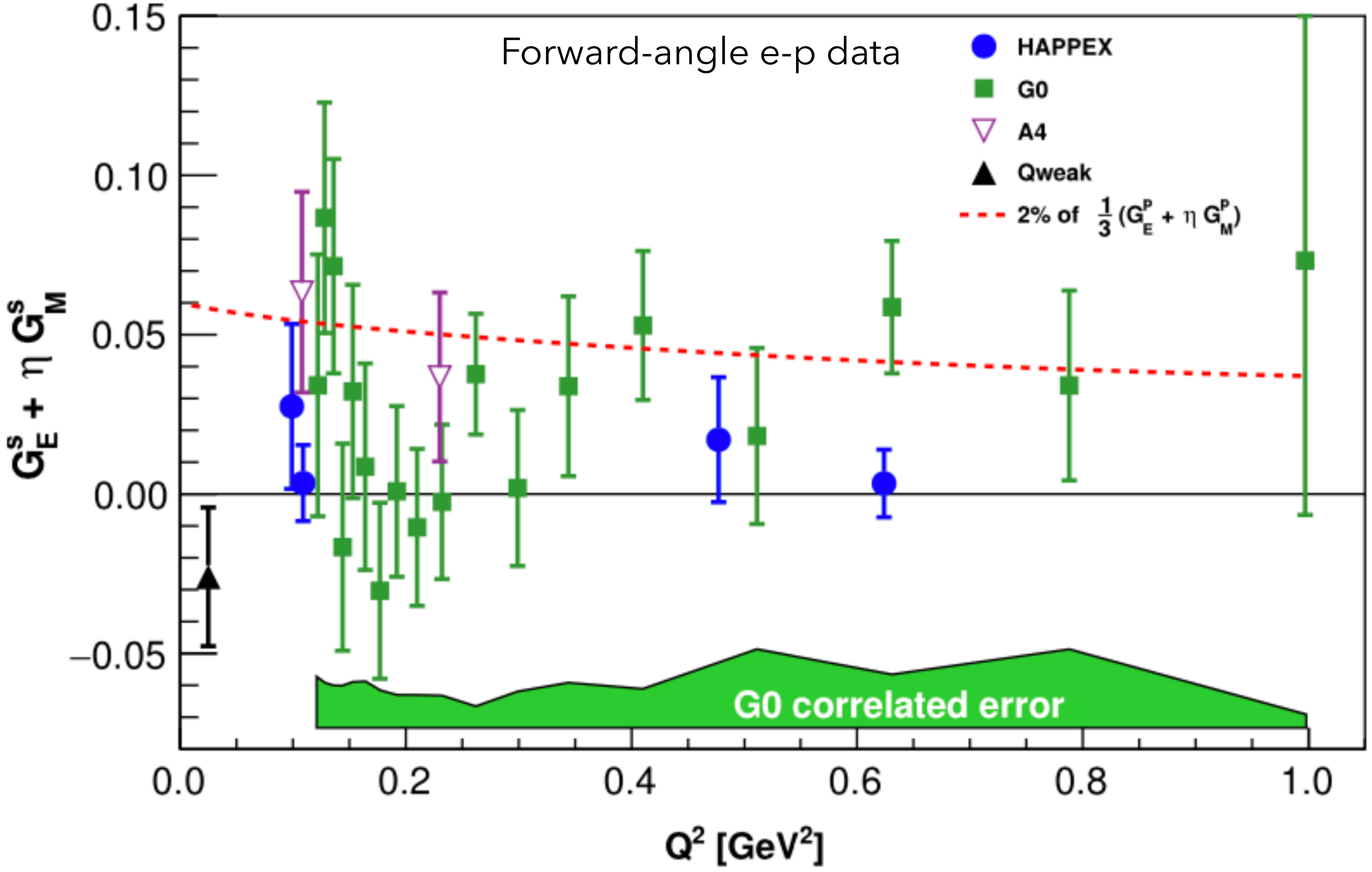

Strange form-factors on the lattice

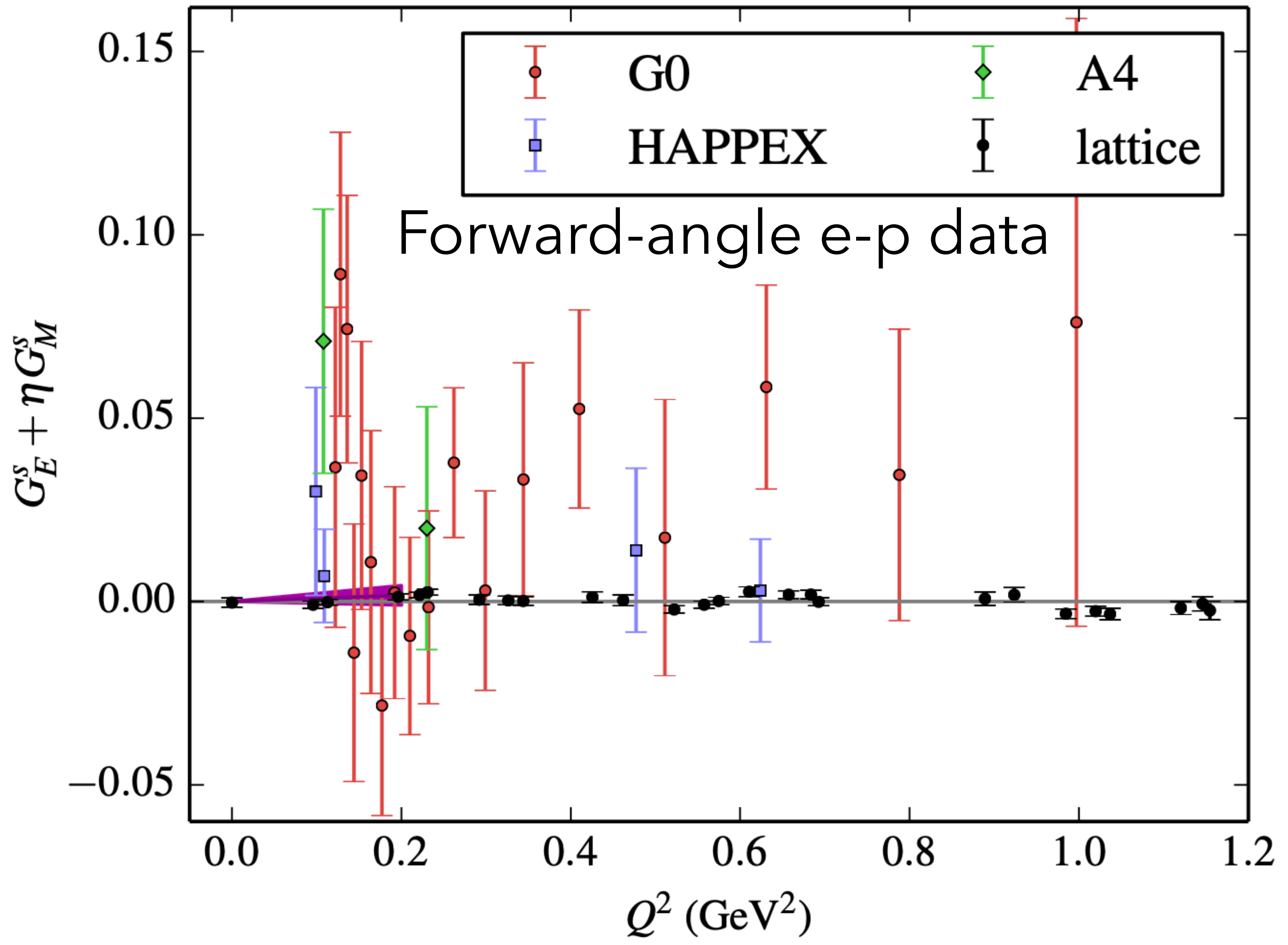

Some lattice calculations predict central values which are small, 10x below the limit of low Q^2 studies.

But they do not apparently fall with Q^2. **These values would be significant contributions at high Q^2**

P. Shanahan *et al.*, PRL 114, 091802 (2015)

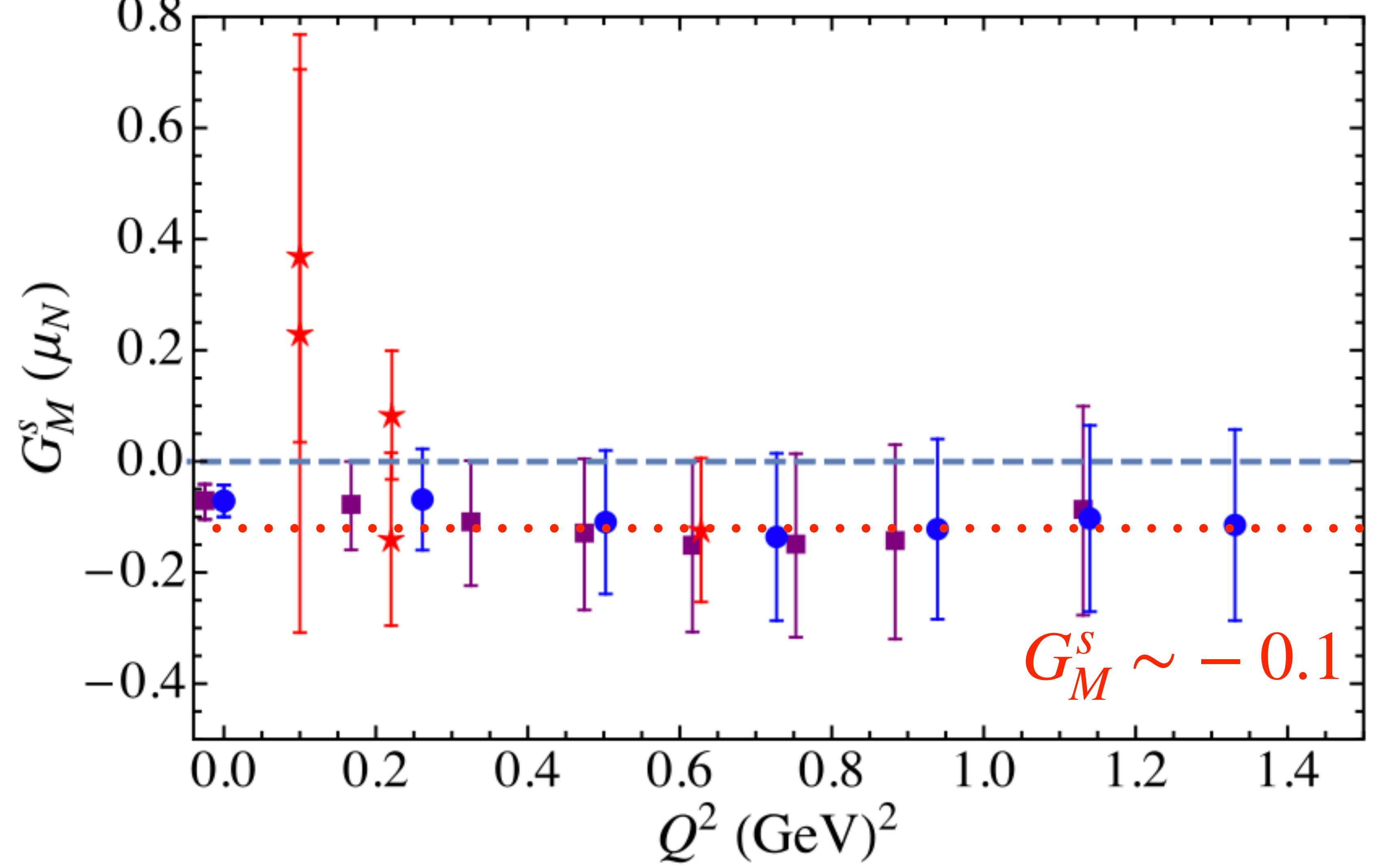

(a)

J. Green *et al.*, Phys. Rev. D 92, 031501 (2015)

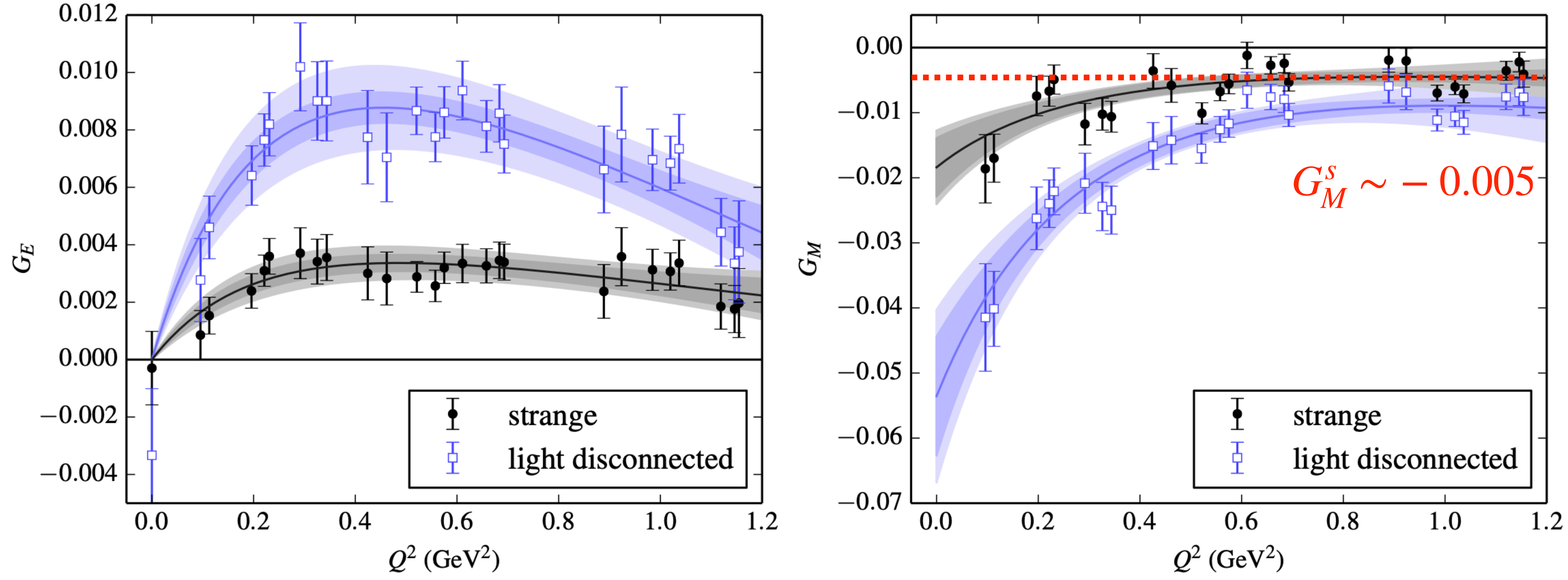

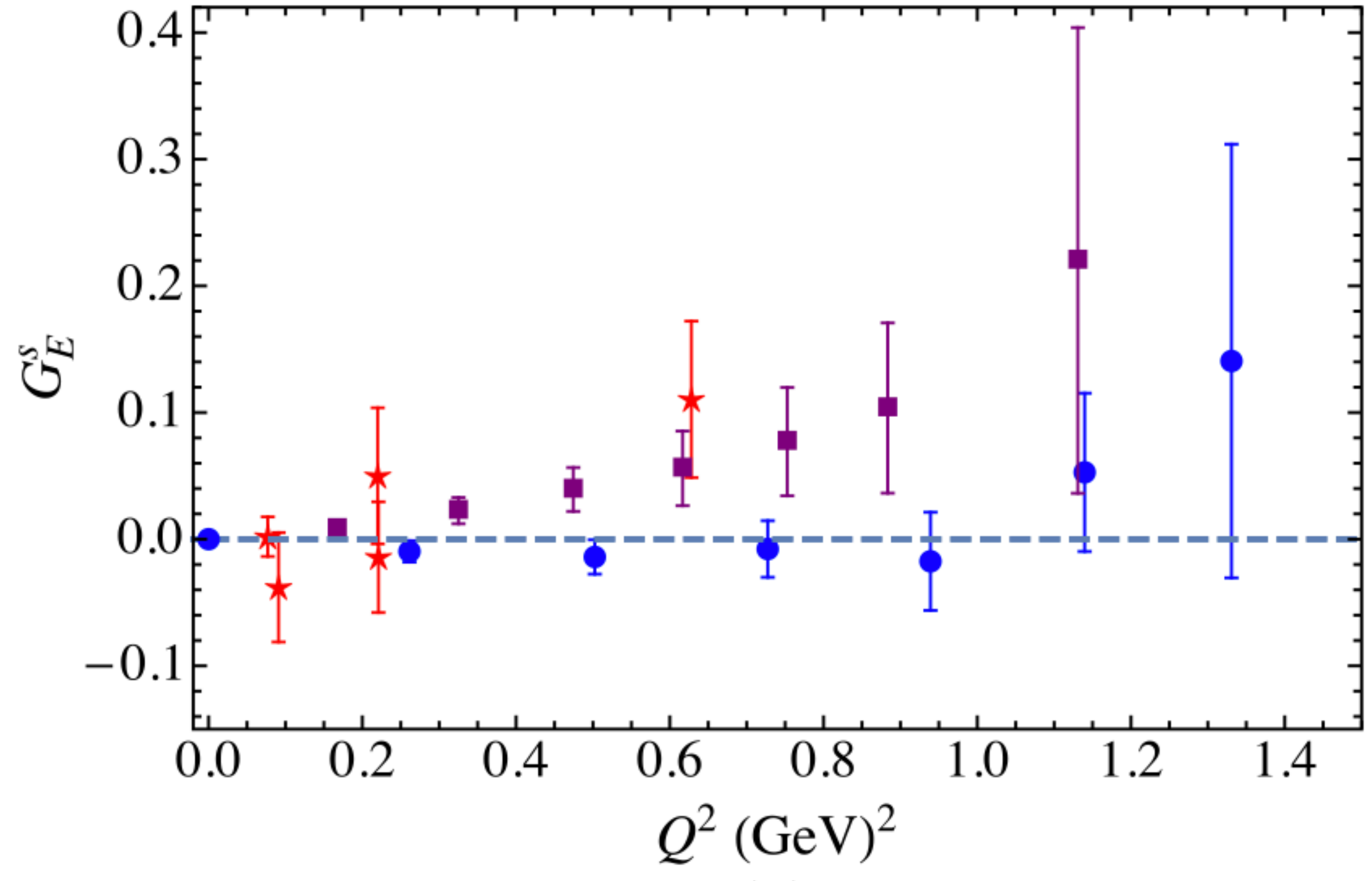

(b)

Strange form-factor predictions

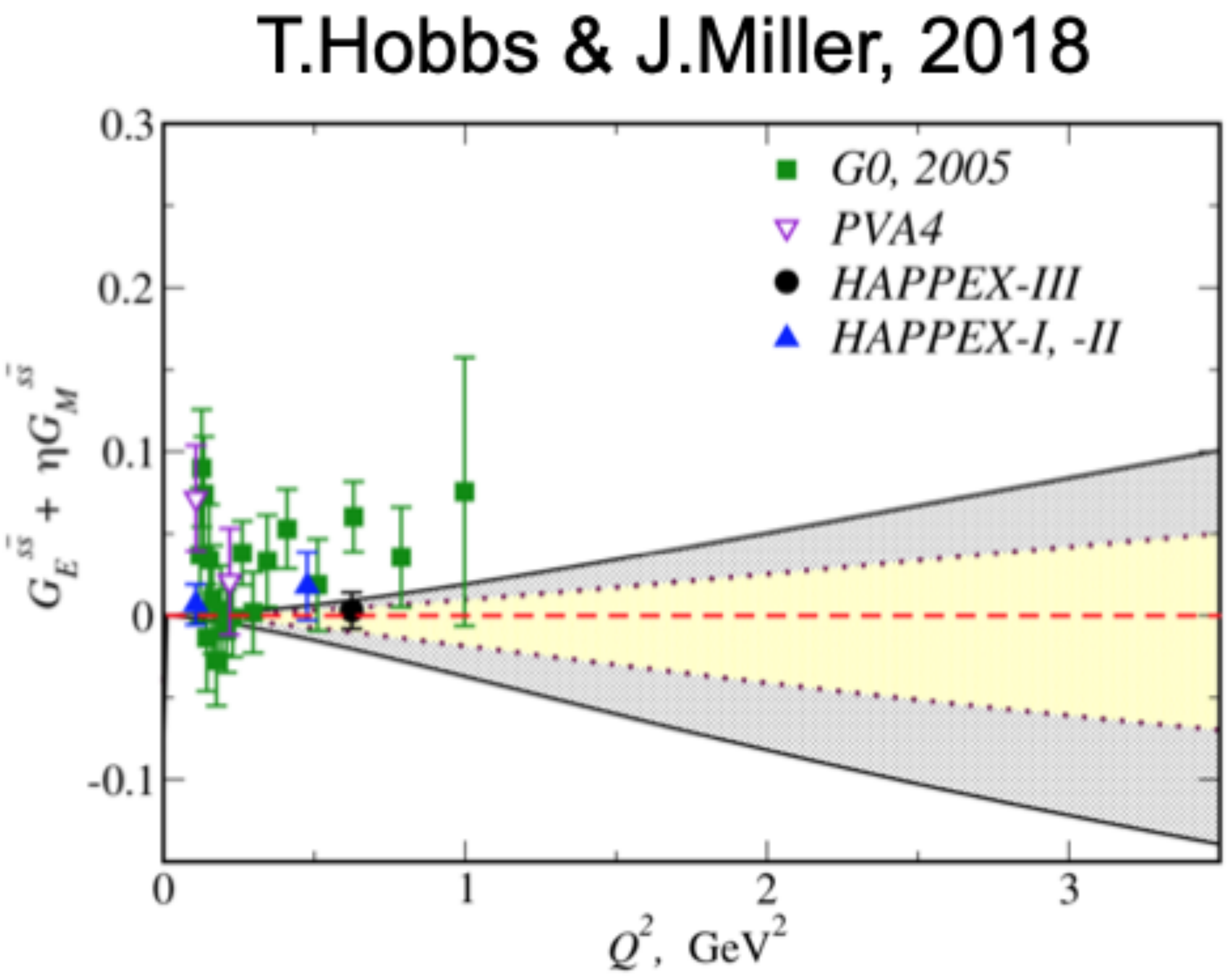

Follows work from *Phys.Rev.C* 91 (2015) 3, 035205
(LFWF to connect DIS and elastic measurements in a simple model)

Conclusion: sFF small (but non-zero) at low Q^2, but quite reasonable within constraints from data to think that they may grow relatively large at large Q^2

To set the scale of the data constraints: the width of the uncertainty band at Q^2 = 2.5 GeV^2 is approximately the size of the dipole form-factor parameterization G_D

G_s/G_D ~ 1 is not excluded

Such a large SFF could be huge in a proton PV measurement
δA_{PV} ~ ±22 ppm, ~±15% of A_{PV}^{ns}

Q^2 dependence of Q^4F_1

$$F_1^u = 2F_{1p} + F_{1n} - F_1^s \qquad F_1^d = 2F_{1n} + F_{1p} - F_1^s$$

Assuming $\delta G^s_{E,M} \sim G_D$ ~ 0.048 $\longrightarrow \delta(Q^4F_1^u)$ ~ ± 0.17

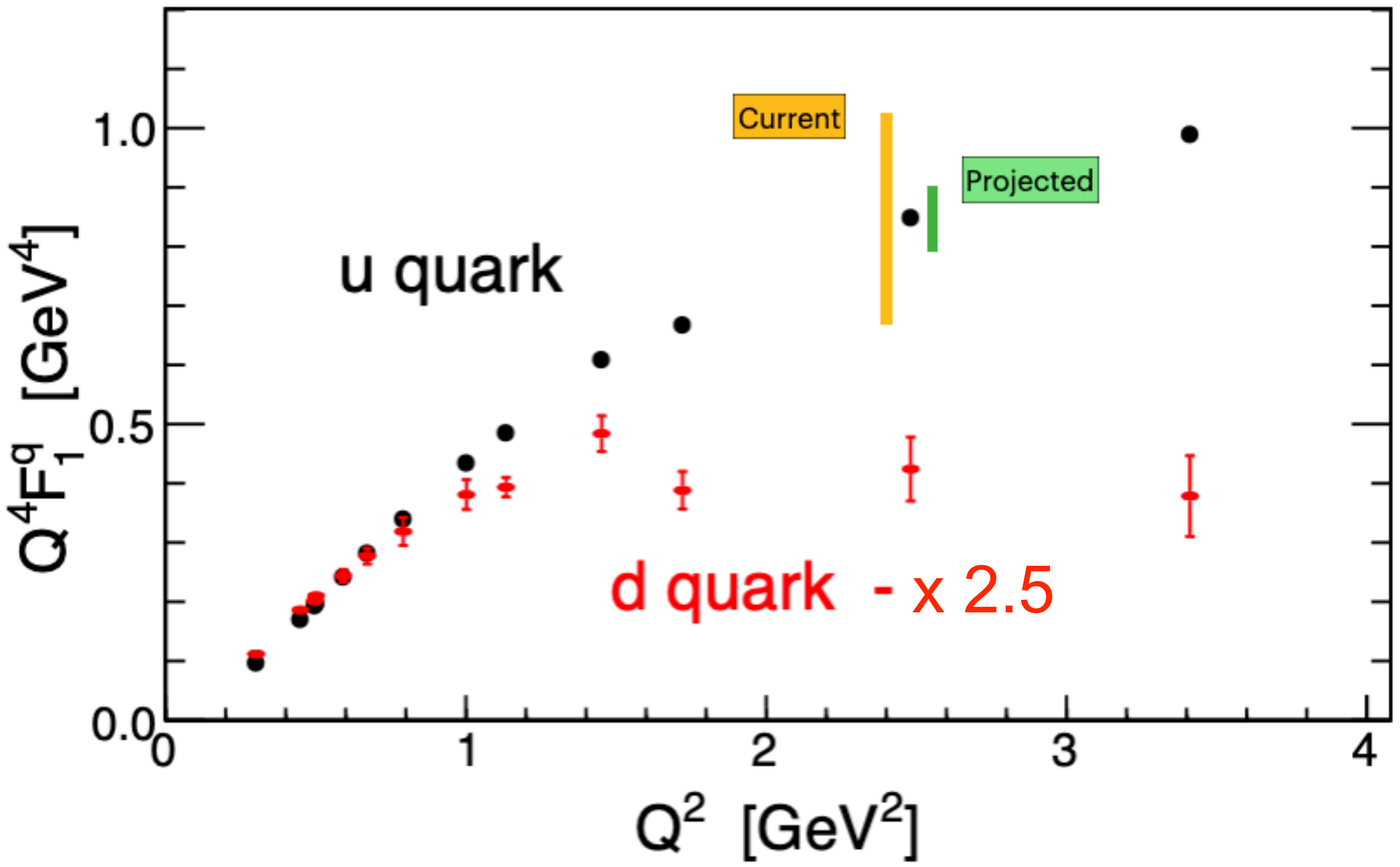

Such a large SFF could be huge in a proton PV measurement
δA_{PV} ~ ±22 ppm, ~±15% of A^{ns}_{PV}

- Flavor separated form factors are a crucial piece of information for GPDs / nuclear femtography.
- So far, these have relied on poorly tested assumptions of strange quark contributions.
- Experimentally not ruled out (at level of yellow band) and lattice calculations do not rule out significant contributions (at level of 1x-2x the green band)

A measurement is needed

The planned measurement

Aim for Q^2 = 2.5 GeV^2

Identify elastic kinematics with electron-proton coincidence

- Angular e-p correlation, 6.6 GeV beam energy
  (electron at 15.5 degrees, proton at 42.4 degrees)
- High resolution calorimeter trigger for electron arm
- Calorimeter trigger for proton arm
- Scintillator array on proton arm, to improve position resolution

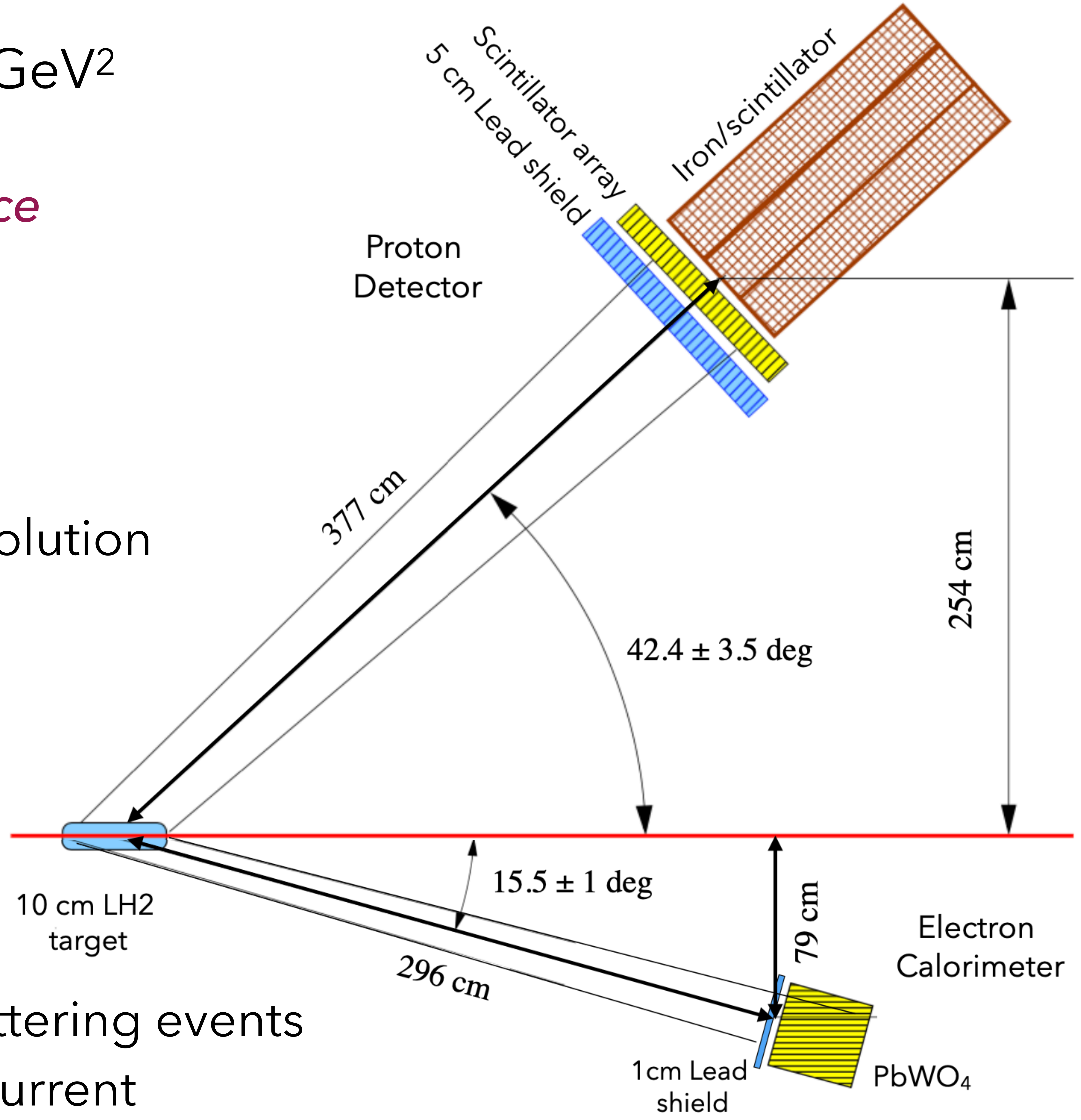

- APV = 150 ppm, 4% precision goal, so 3×10^{10} elastic scattering events
- $\mathcal{L} = 1.7 \times 10^{38}\ cm^{-2}/s$, 10 cm LH_2 target and 65 µA beam current
- Full azimuthal coverage, ~42 msr

Calorimeters reusing components

NPS electromagnetic calorimeter

- 1200 $PBWO_4$ scintillators, PMTs + bases

SBS hadronic calorimeter

- 288 iron/scintillator detectors, PMTs + bases

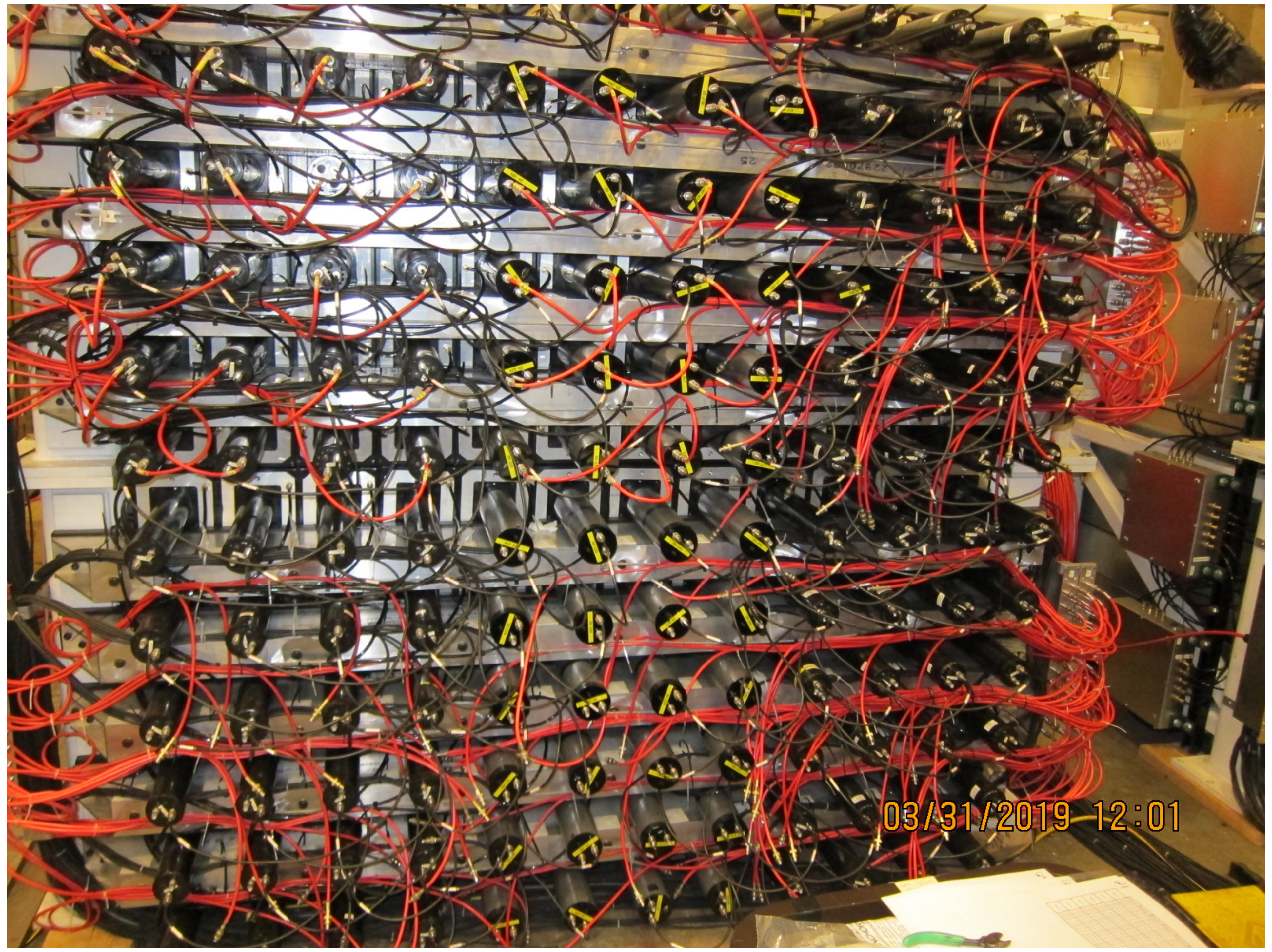

Detector System

HCAL - hadron calorimeter
- Detector elements from the SBS HCAL
- 288 blocks, each 15.5 x 15.5 x 100 cm^3
- iron/scintillator sandwich with wavelength shifting fiber readout

ECAL - electron calorimeter
- Detector elements from the NPS calorimeter
- 1200 blocks, each 2 x 2 x 20 cm^3
- $PbWO_4$ scintillator

Scintillator array
- 7200 plastic scintillators, each 3 x 3 x 10 cm^3
- Wavelength shifting fiber to MA-PMT
- Used for position resolution in front of HCAL

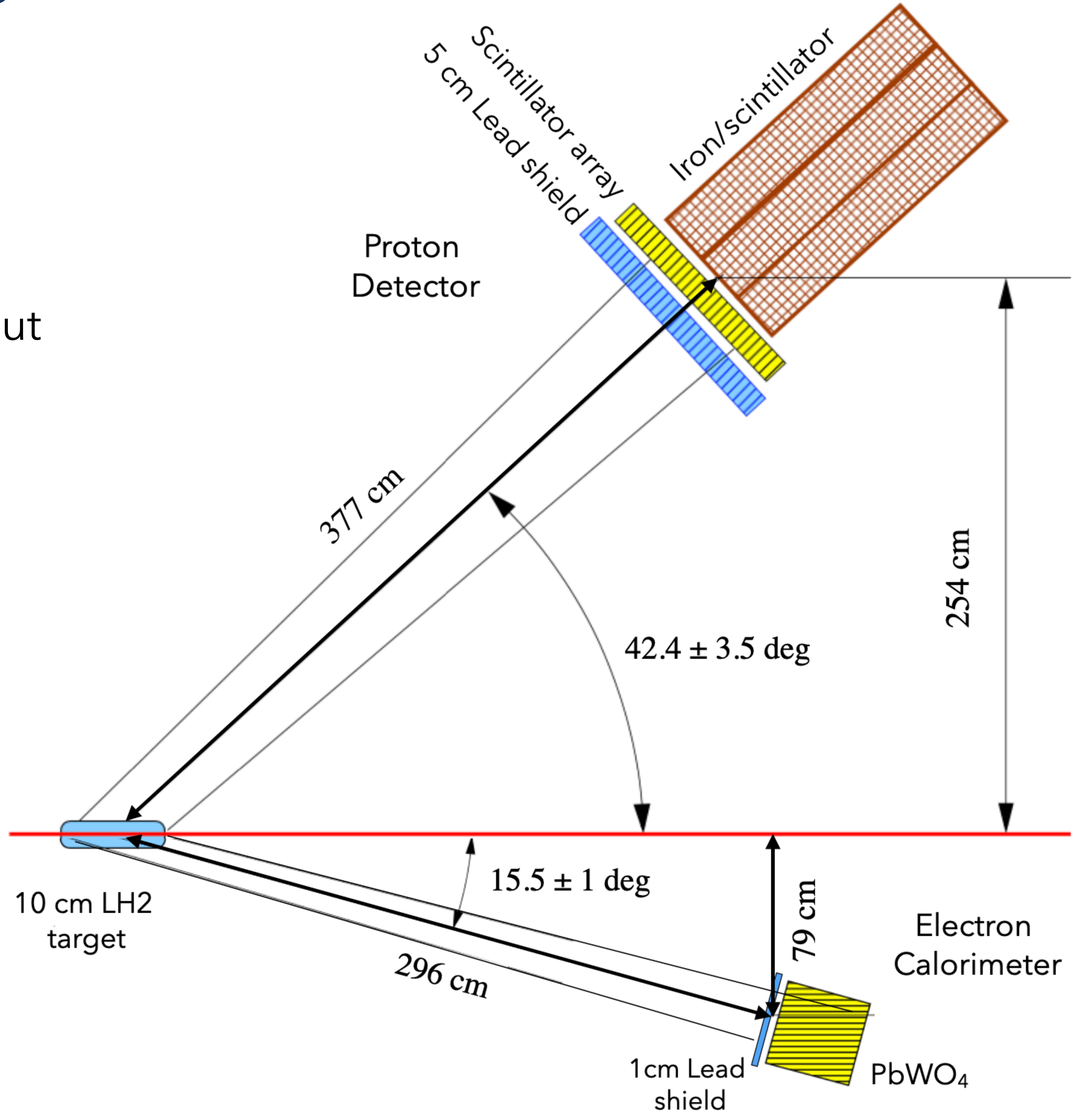

Experimental concept

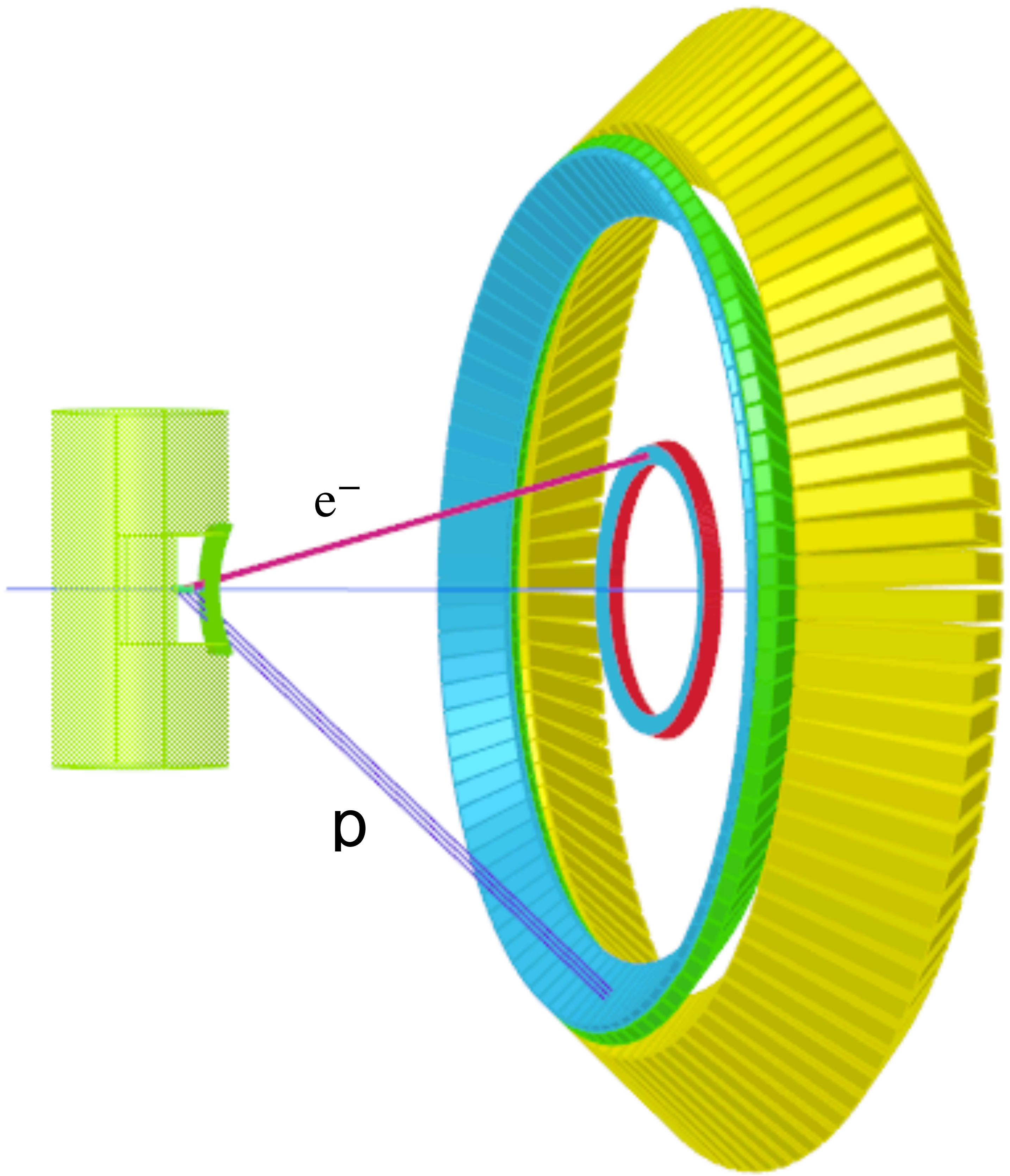

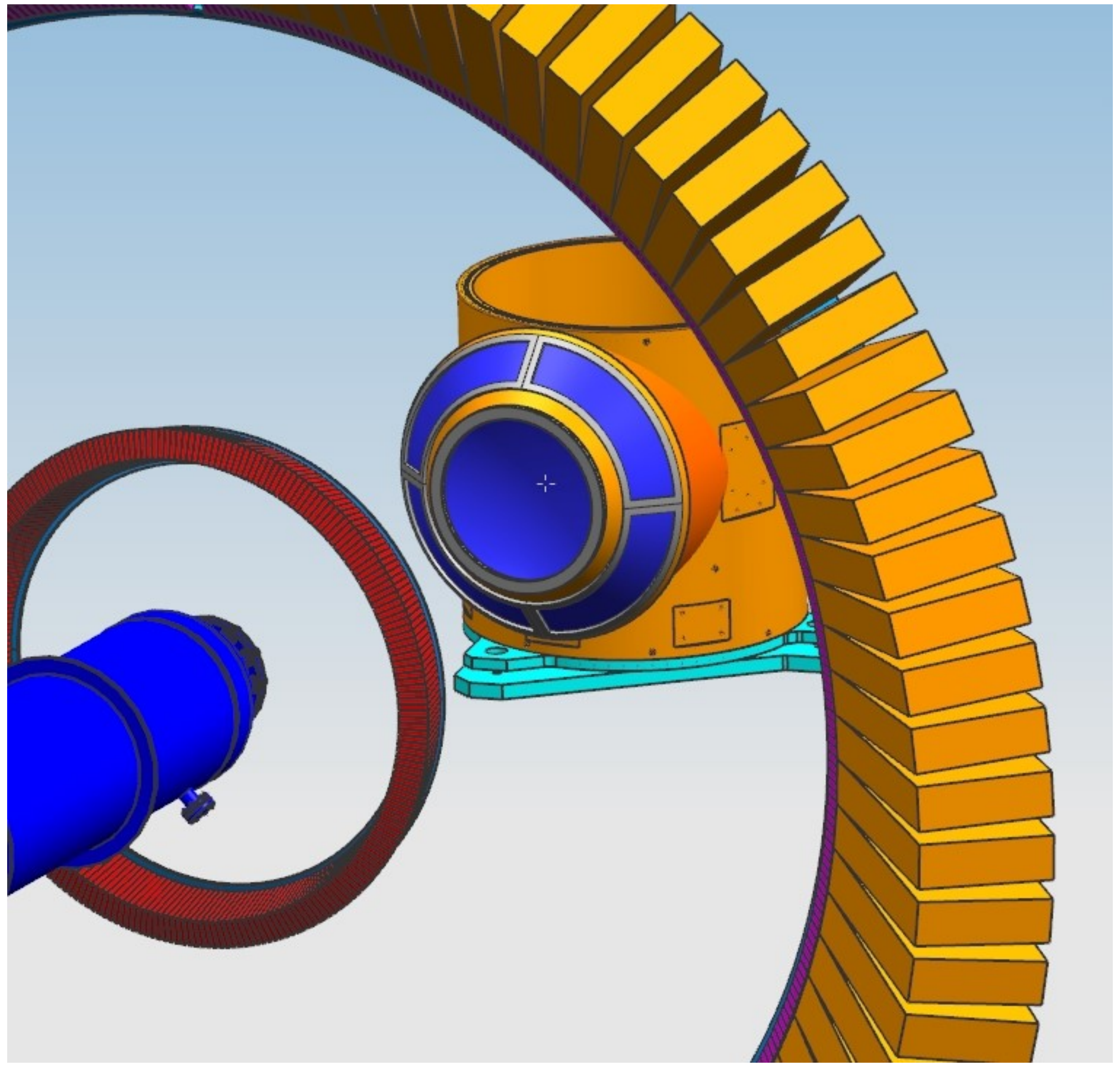

Preliminary design of scattering chamber

He bag will reduce backgrounds between target chamber and exit beampipe

This fits in Hall C (but it's tight)

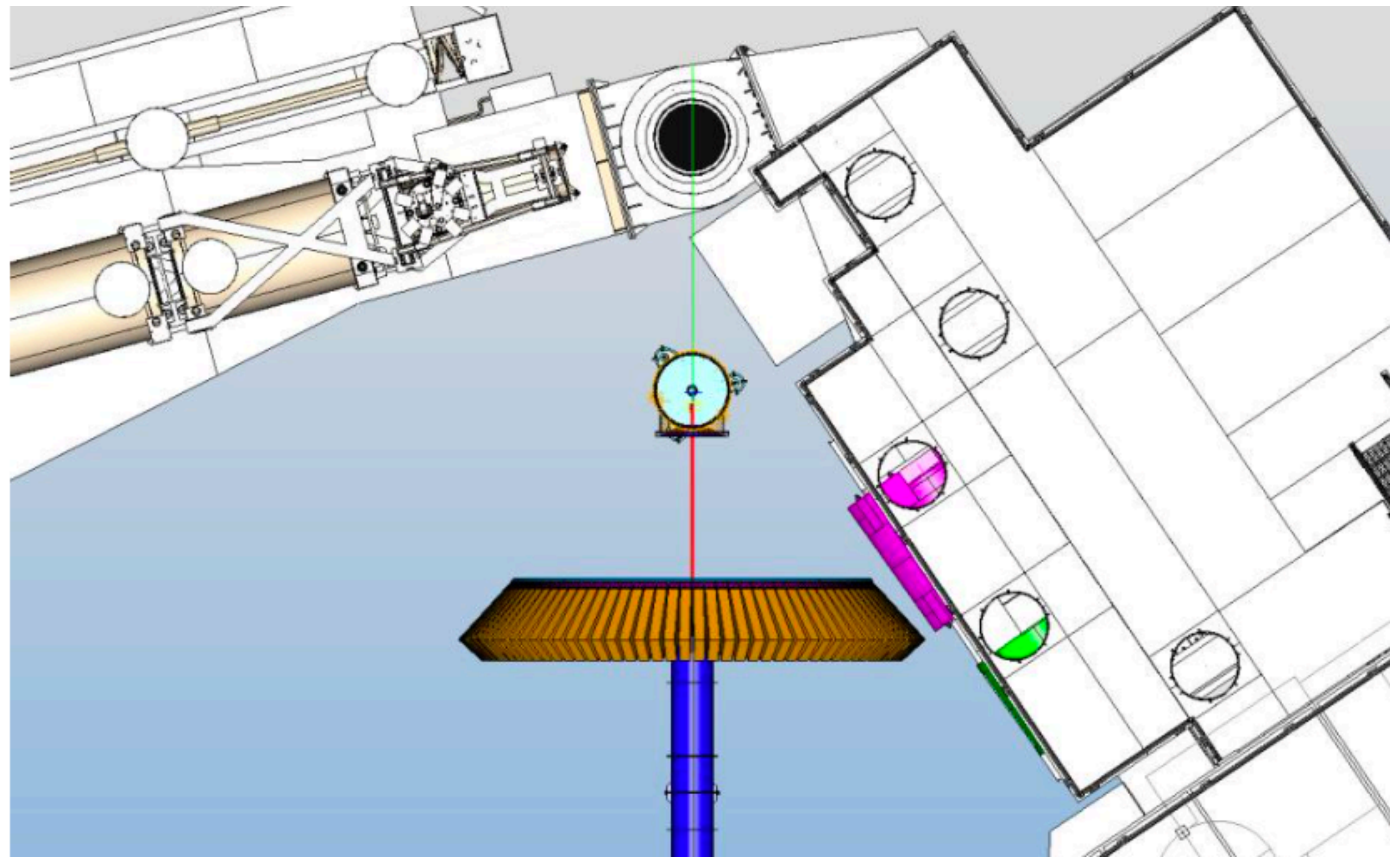

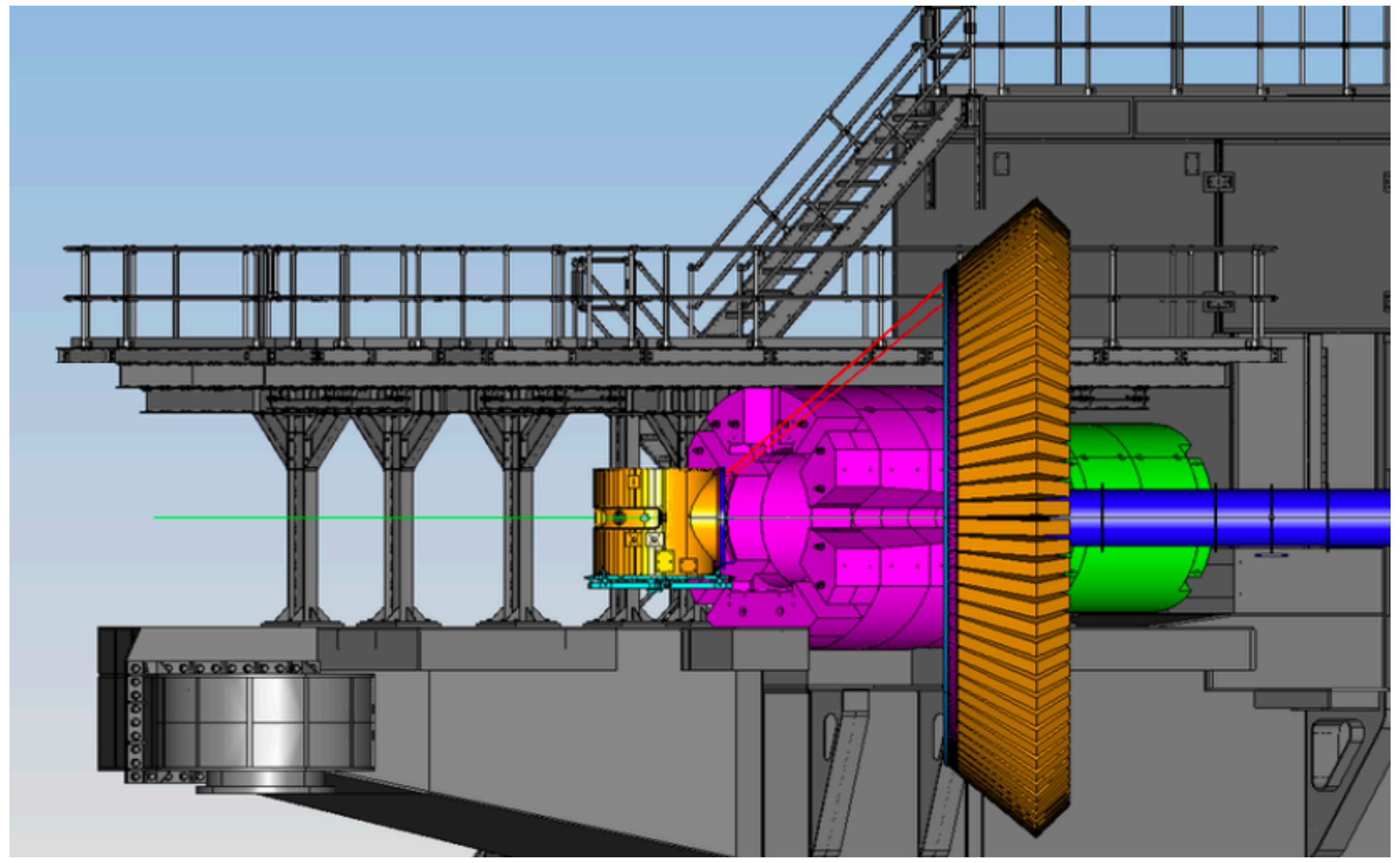

Trigger: calorimeters, with geometric coincidence

A relatively high ECAL cut (~66% of beam energy) and loose e-p coincidence cut provides high efficiency and manageable data rate

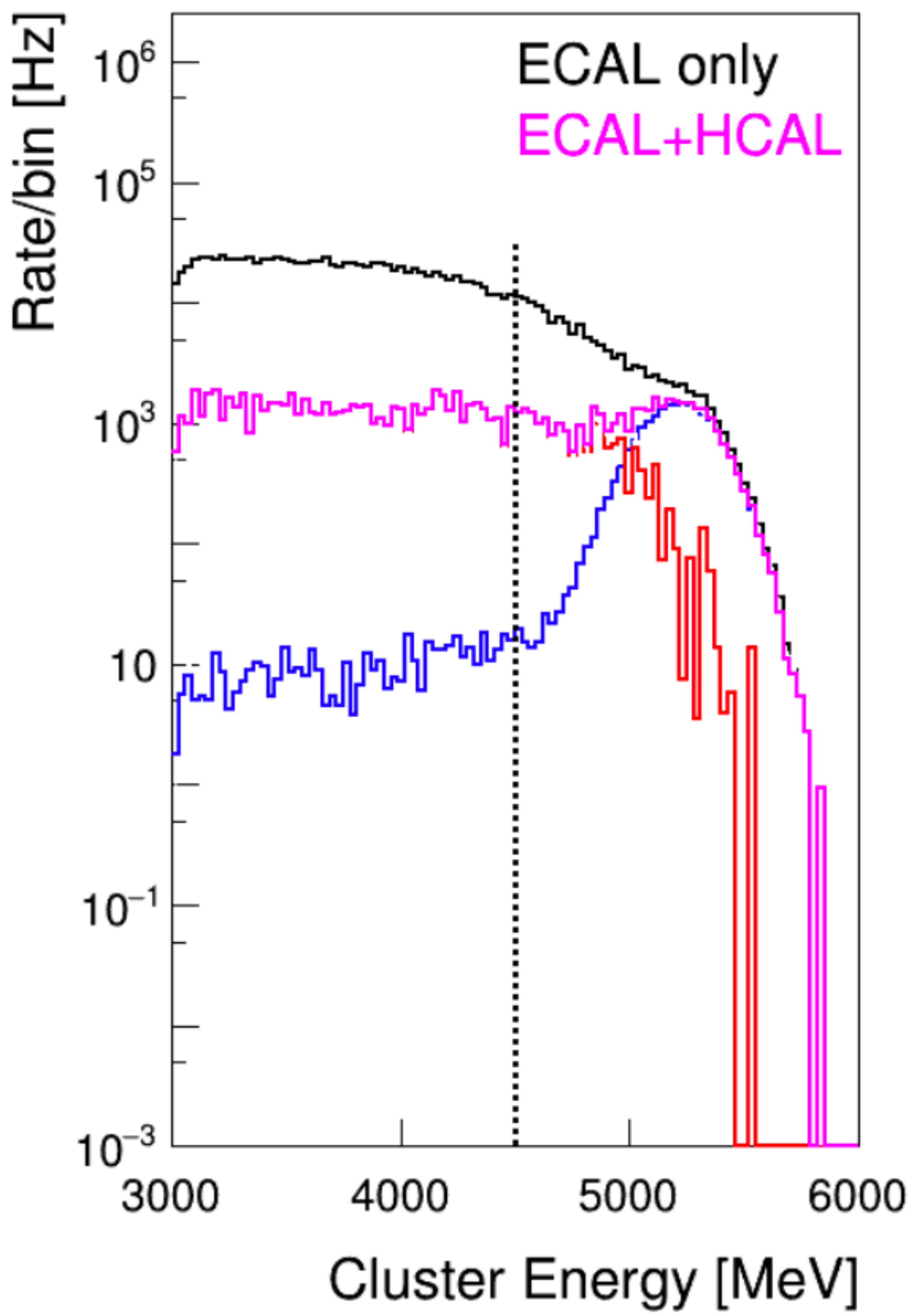

ECAL > 4.5 GeV: 150 kHz

ECAL + HCAL in coincidence: 35 kHz

Fraction of total by event type	Online
Elastic scattering	0.531
Inelastic (pion electro-production)	0.450
Quasi-elastic scattering (target windows)	0.015
π^0 photo-production	0.004

Elastic event discrimination

Azimuthal angle

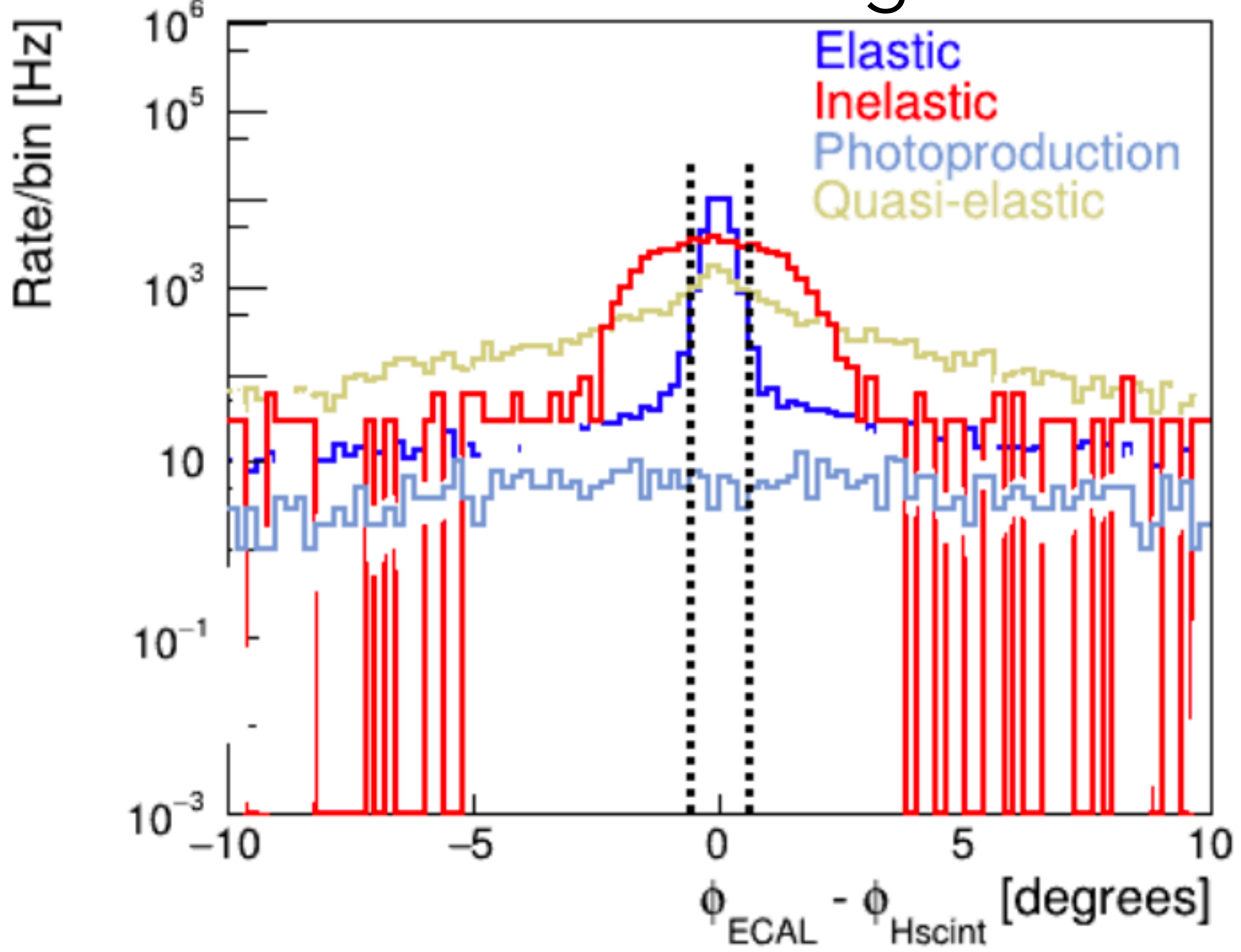

dashed lines = offline cuts

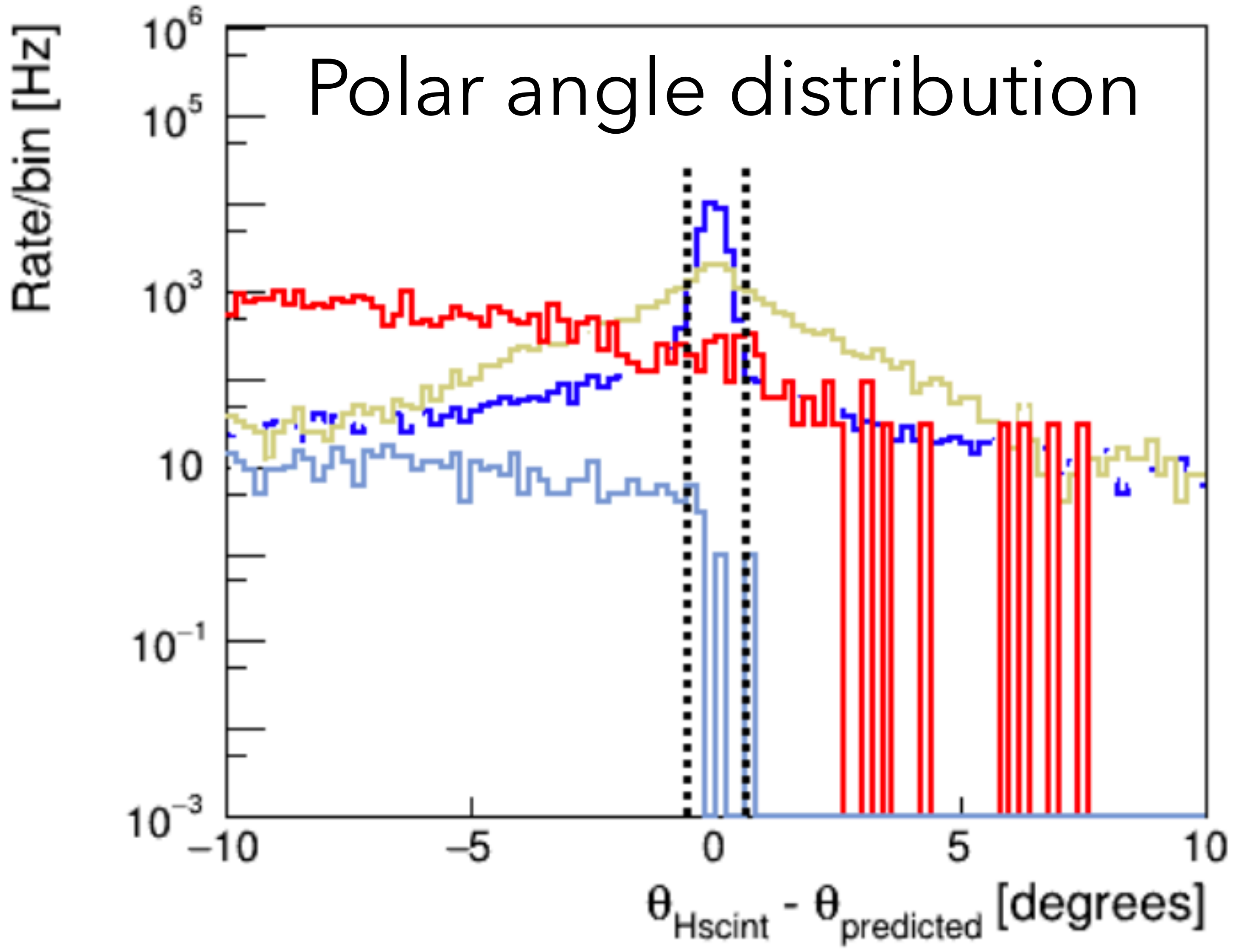

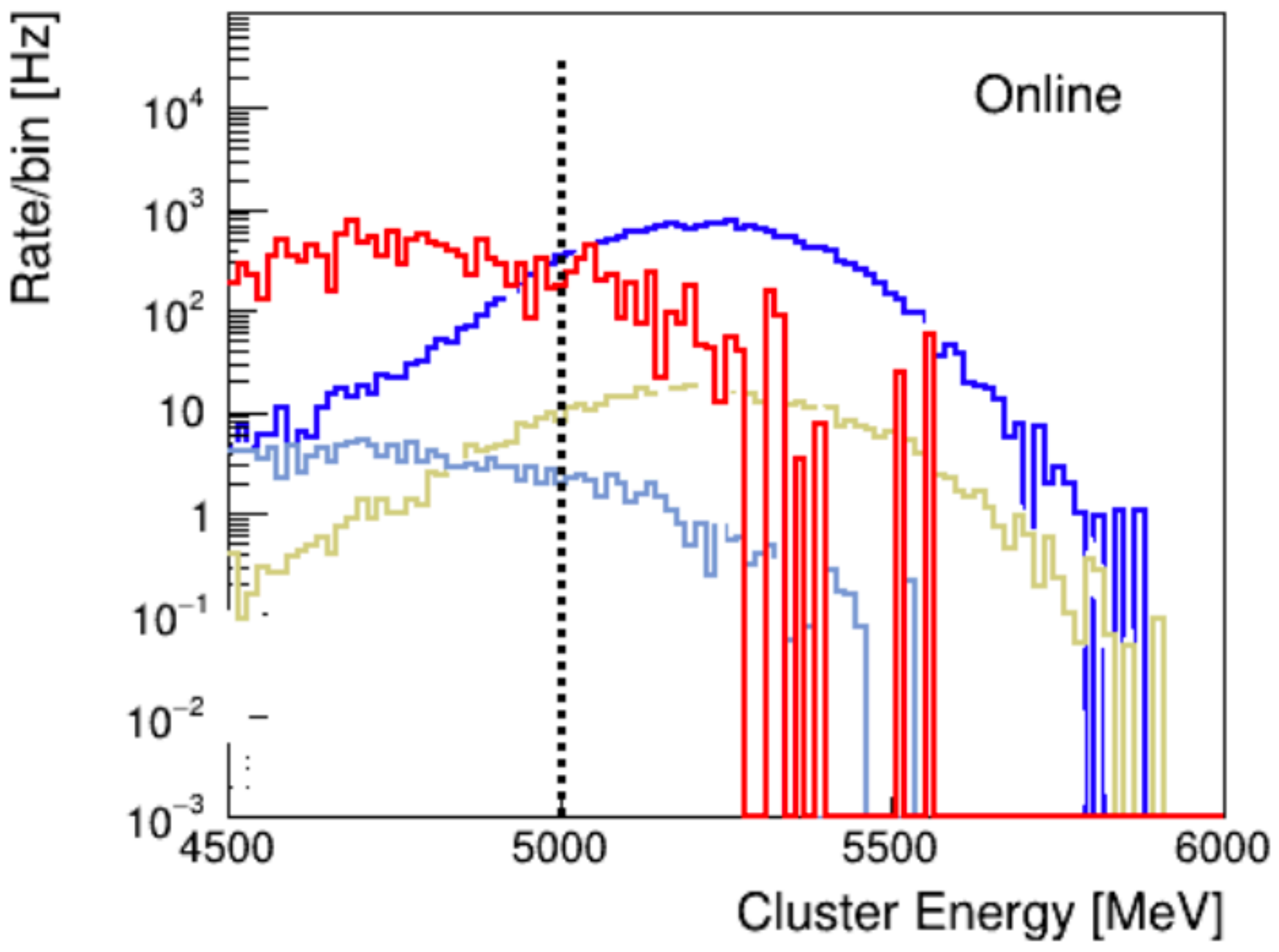

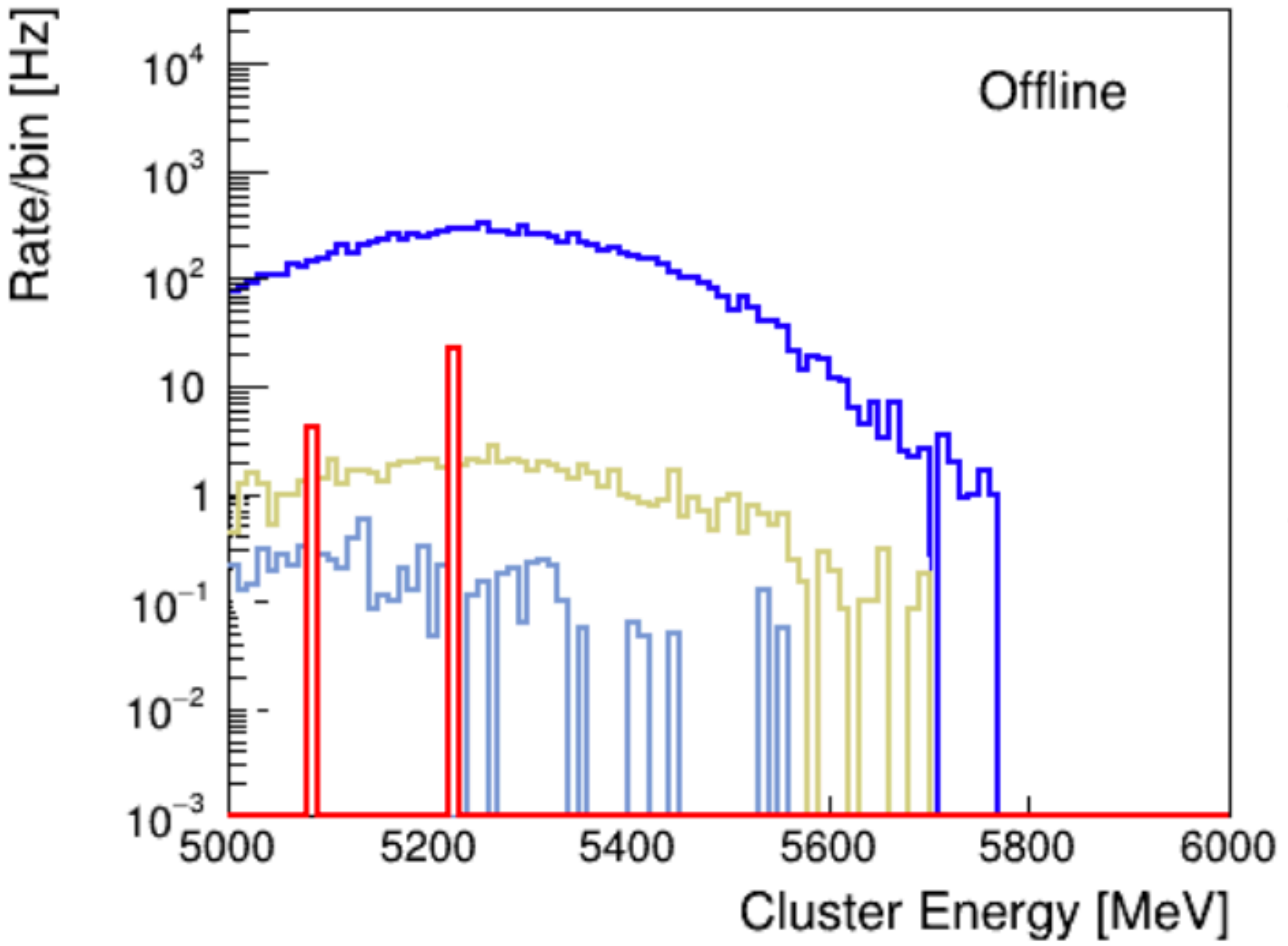

Offline: tighten geometric cut with pixel hodoscope and ECAL cluster center

Exclude inelastic background to ~0.2%

Fraction of total by event type	Offline
Elastic scattering	0.989
Inelastic (pion electro-production)	0.002
Quasi-elastic scattering (target windows)	0.008
π^0 photo-production	0.001

"sideband" analyses will help verify QE and inelastic asymmetries

Projected result

A_{PV} = 150 ppm (if no strange FF)

δA_{PV} = ± 6.2 (stat) ± 3.3 (syst) ($\delta A/A$ = ± 4% ± 2%)

$$\delta\left(G_E^s + 3.1 G_M^s\right) = \pm\ 0.013\ \text{(stat)}\ \pm\ 0.007\ \text{(syst)} = 0.015\ \text{(total)}$$

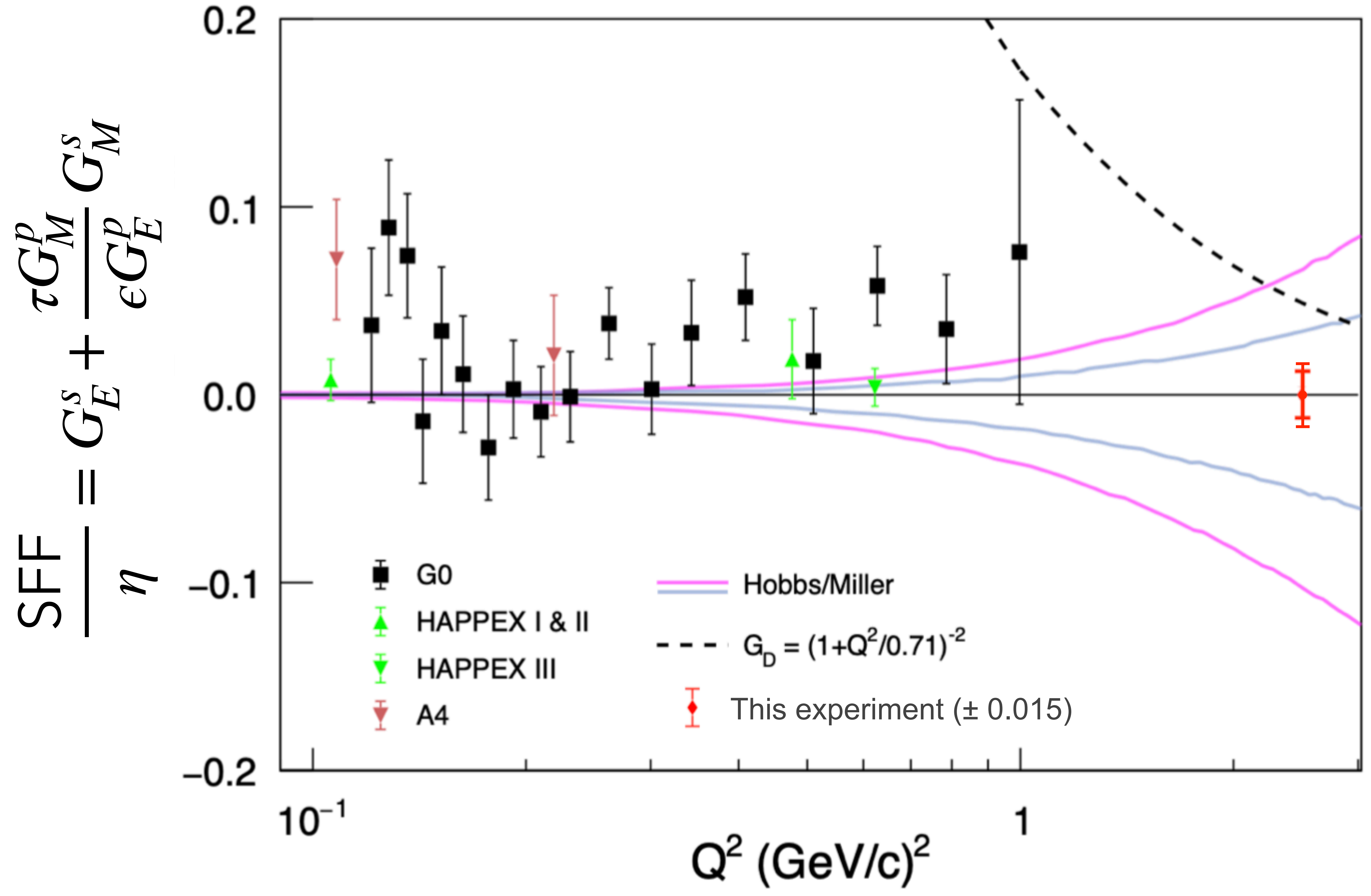

If $G_M^s = 0$, $\delta G_E^s \sim 0.015$, (about 34% of G_D)

If $G_E^s = 0$, $\delta G_M^s \sim 0.005$, (about 11% of G_D)

The proposed measurement is especially sensitive to G_M^s

The proposed error bar reaches the range of lattice predictions, and the empirically unknown range is much larger.

Next Step - Test Performance of Detector Concept

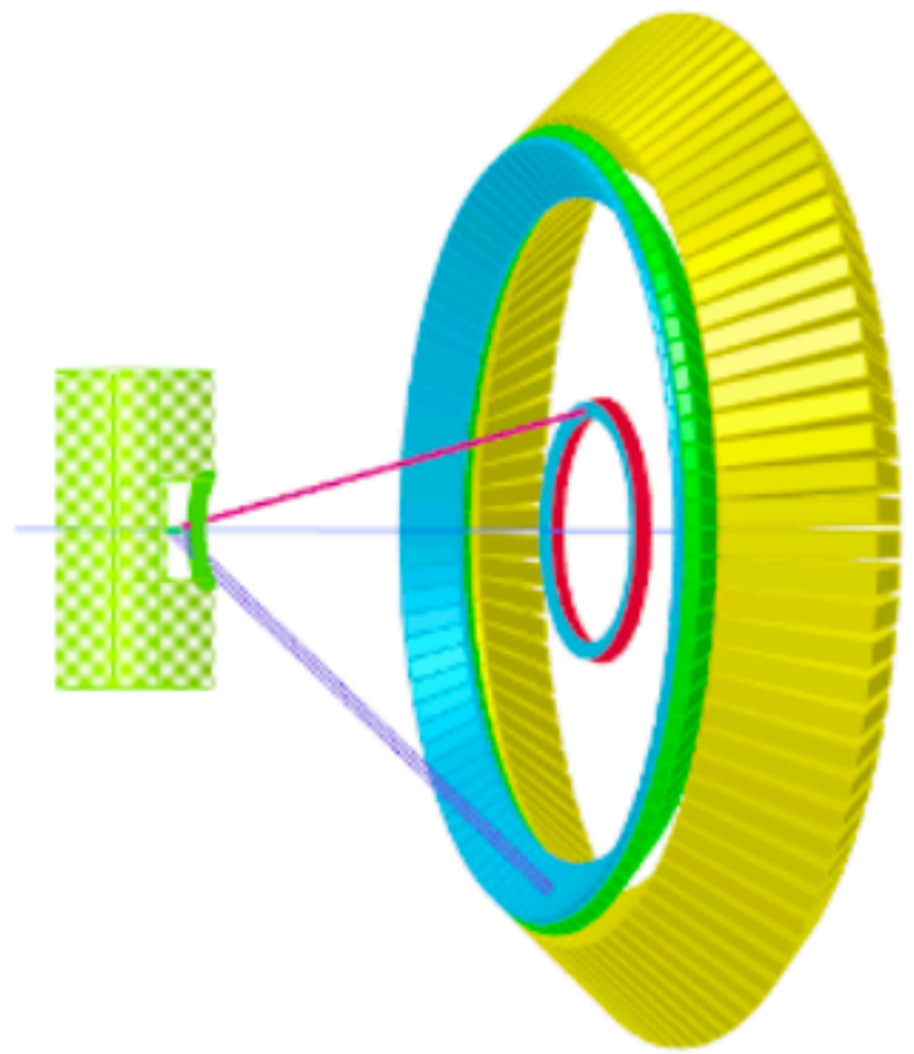

electron angle 15.5°
proton angle 42.4°

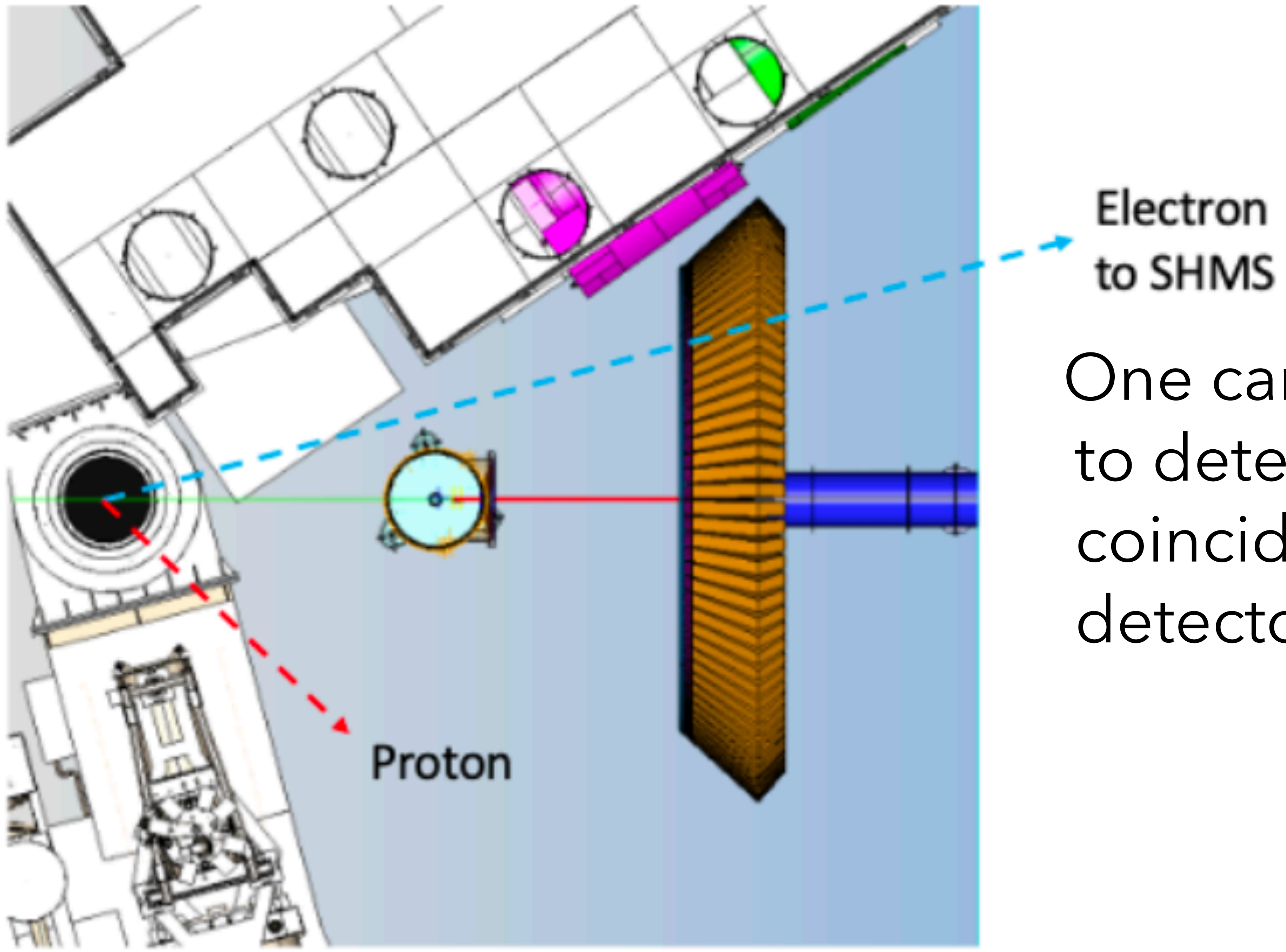

One can position the SHMS to 15.5° to detect electrons, measured in coincidence with a prototype proton detector at 42.4°

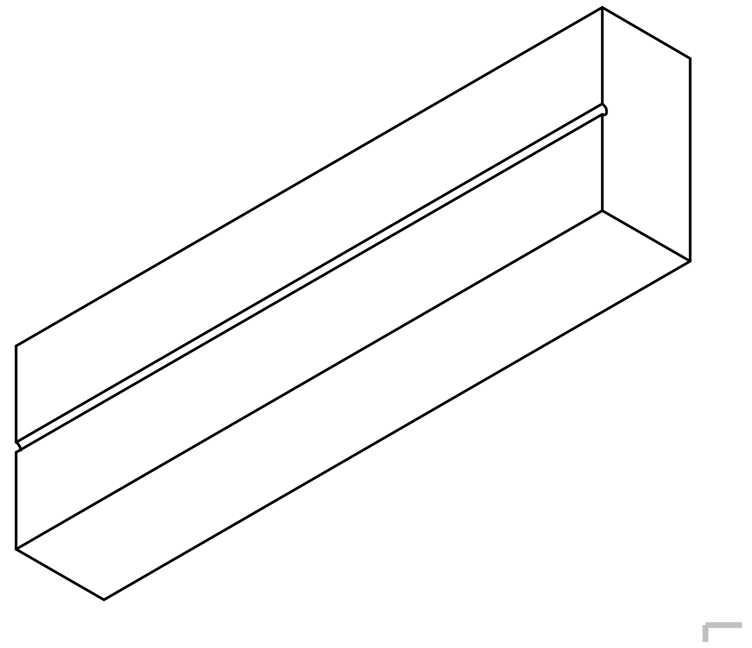

Prototype proton detector:

- pixel array of 32 small scintillators with MA-PMT readout with 6 SBS HCAL blocks
- NINO card front-end, FADC readout
- 50uA on 15cm Hydrogen target at 6.6 GeV, about 2kHz rate into detector
- test elastic identification and background rate

LaTech has purchased scintallators, to be glued with WLS fibers for prototype this summer

Error budget

quantity	value	contributed uncertainty
Beam polarization	85% ± 1%	1.2%
Beam energy	6.6 + / − 0.003 GeV	0.1%
Scattering angle	$15.5^\circ \pm 0.03^\circ$	0.4%
Beam intensity	<100 nm,<10 ppm	0.2%
Backgrounds	< 0.2 ppm	0.2%
G_E^n/G_M^n	-0.2122 ± 0.017	0.9%
G_E^p/G_M^p	0.246 ± 0.0016	0.1%
σ_n/σ_p	0.402 ± 0.012	1.2%
$G_A^{Zp}/G_{\text{Dipole}}$	-0.15 ± 0.02	0.9%
Total systematic uncertainty:		2.2%

or 3.3 ppm

Statistical precision for A_{PV}: 6.2 ppm (4.1%)

Radiative correction uncertainties are small; theoretical correction uncertainty lies in the proton "anapole" moment

If the anapole uncertainty is not improved, this would contribute at additional 4.1 ppm (2.7%) uncertainty

Summary

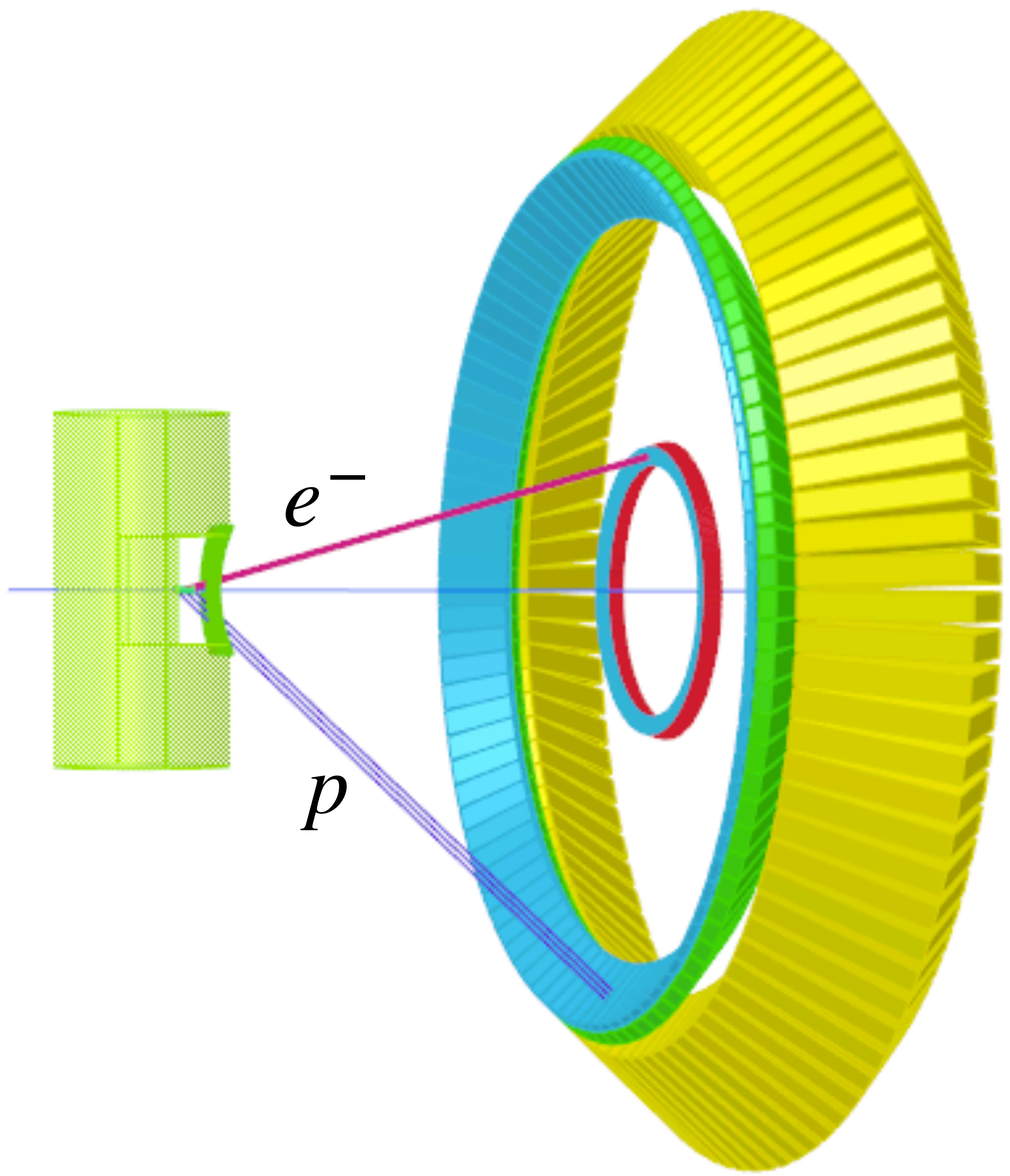

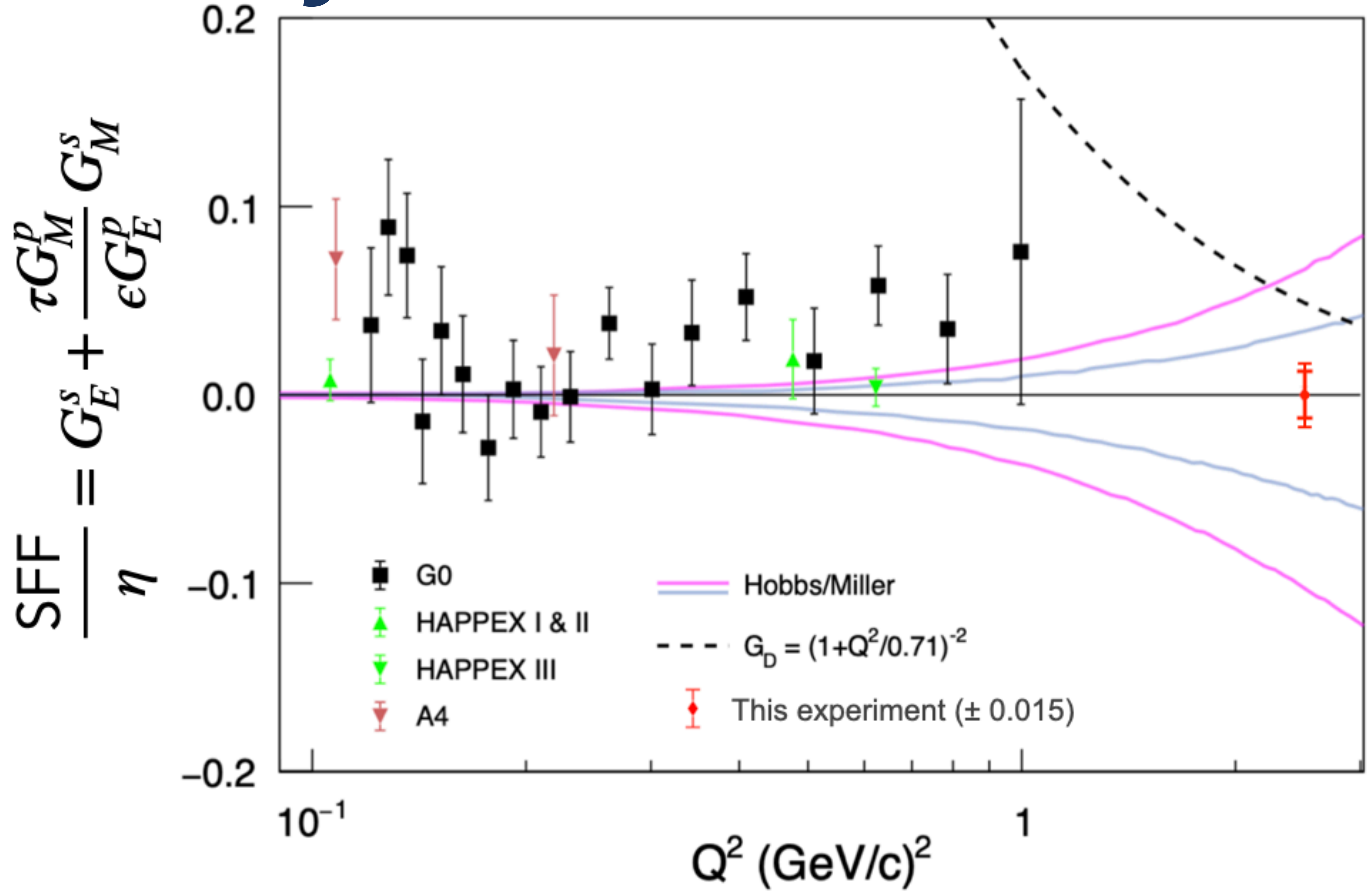

- 10+ years after the last sFF searches were performed, a new experiment is now planned for much higher Q^2, motivated by interest in flavor decomposition of electromagnetic form factors
- Projected accuracy at ~11% of the dipole value allows high sensitivity search for non-zero strange form factor.
- The proposed error bar is in the range possibly suggested by lattice predictions, and significantly smaller than the uncertainty range in the extrapolation from previous strange form-factor data
- PAC approved, but needs funding and development. The path forward is clear.

Backup slides

Beam Time

Configuration #	Procedure	Beam current, μA	time, days
C1	Beam parameters	1-70	1
C2	Detector calibration	10	2/3
C3	Dummy target data	20	1/3
C4	Moller polarimetery	1-5	3
C5	A_{PV} data taking	60	40
	Total requested time		45

Scintillator Array

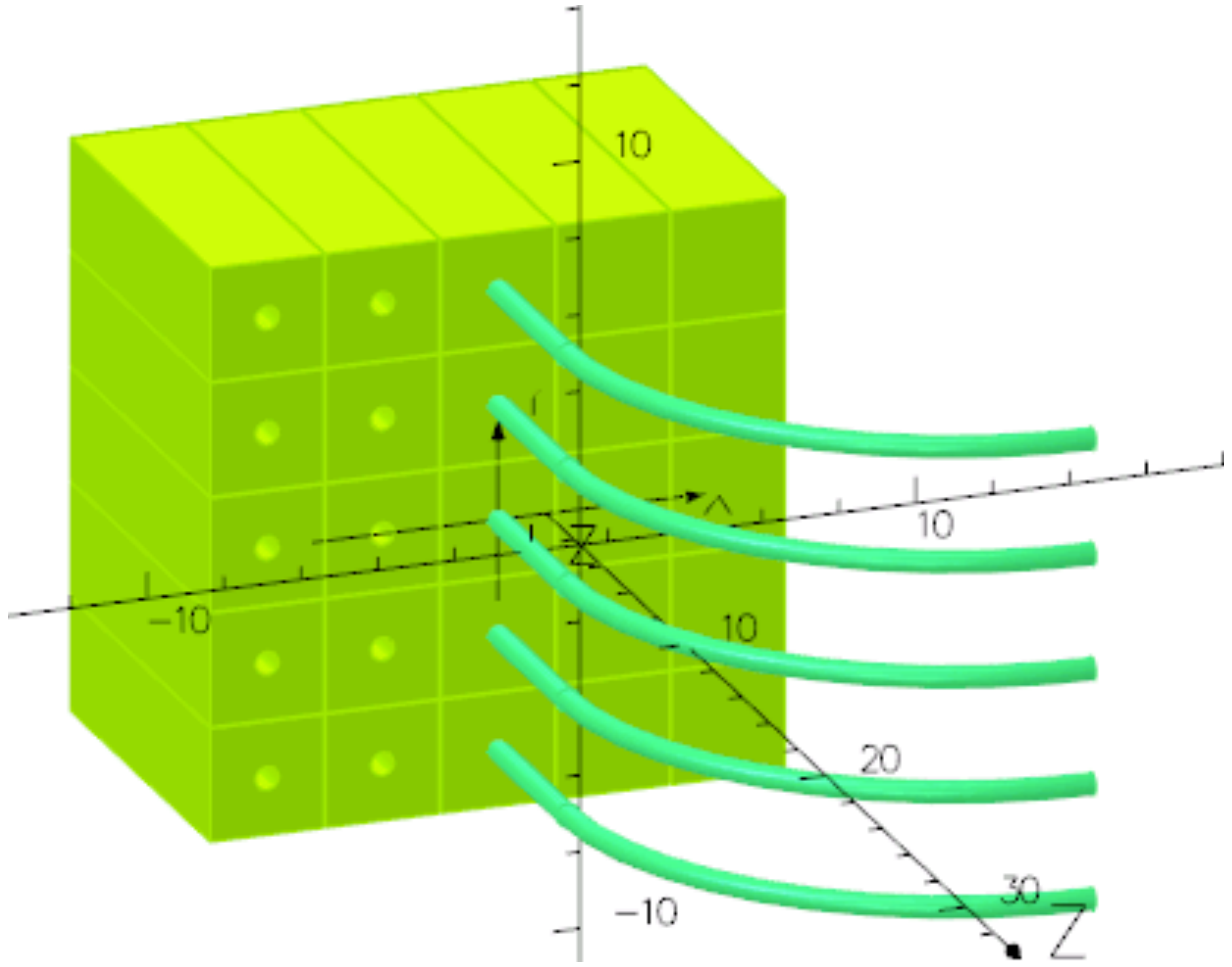

New detector, must be built for this experiment

- Extruded plastic scintillator block
- Readout with wavelength-shifting fiber
- Each fiber read by pixel on multi-anode PMT
- 7200 blocks, each 3 x 3 x 10 cm^3
- Pipeline TDC readout (VETROC)

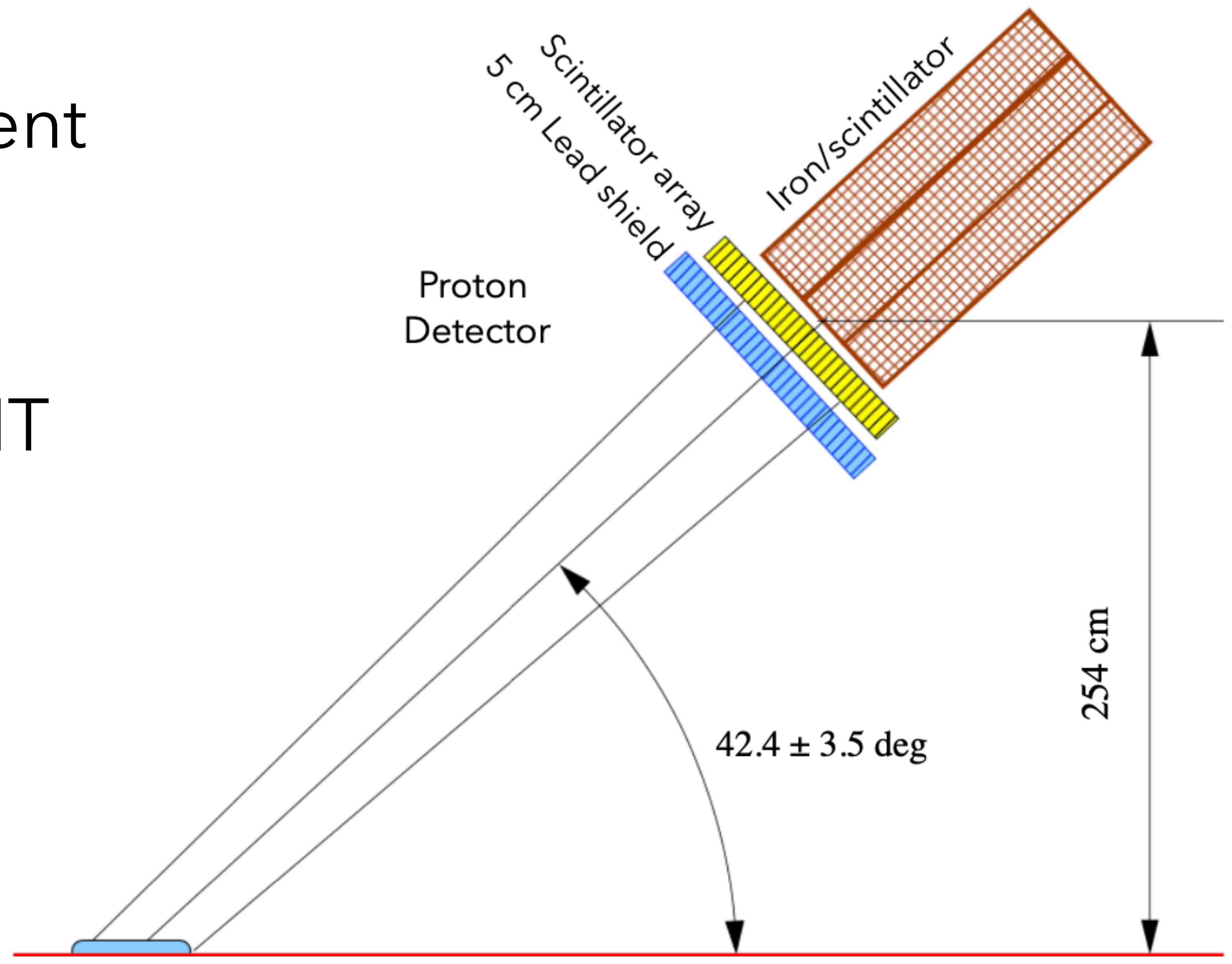

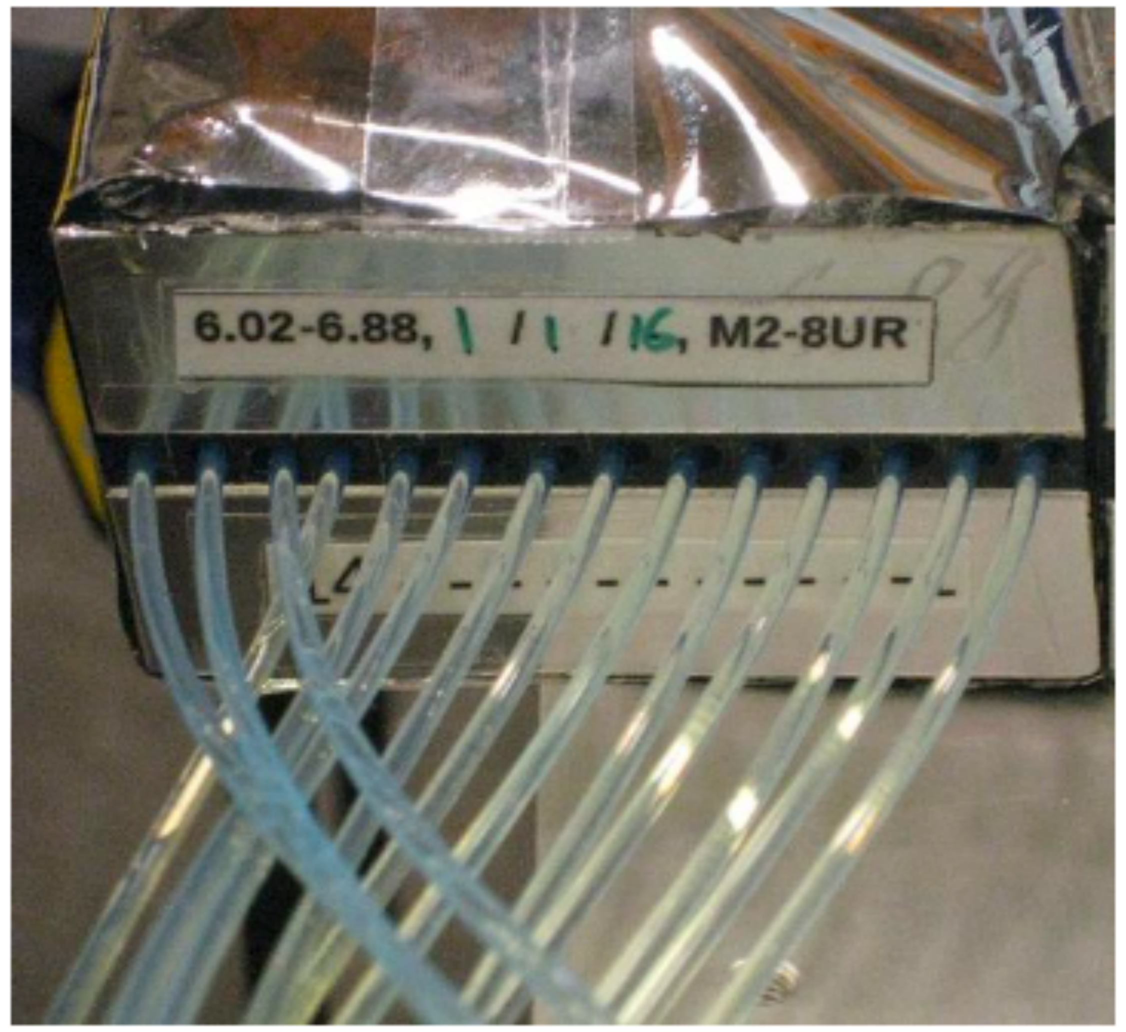

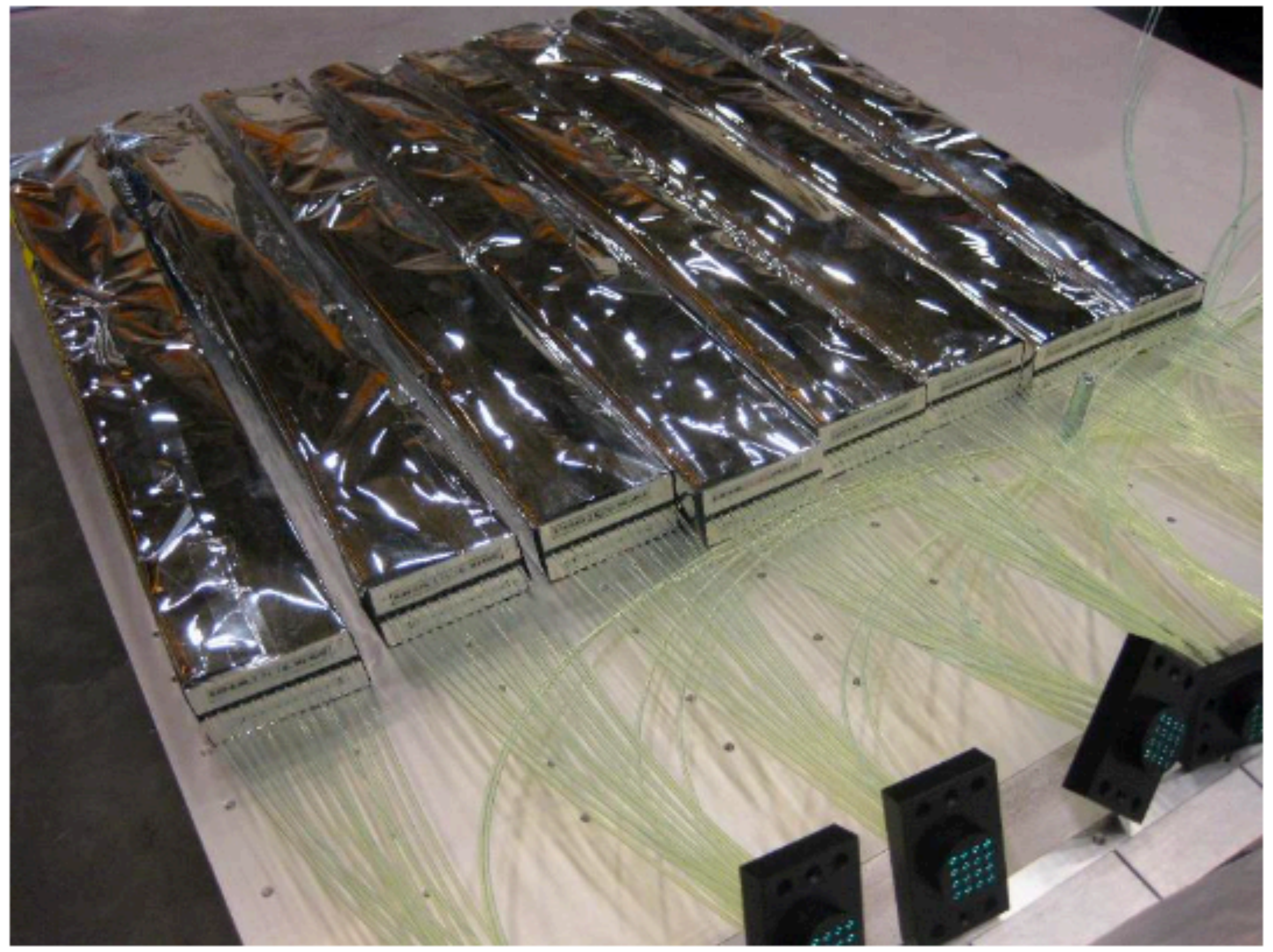

Triggering

Group calorimeter elements into logical "subsystems" for energy threshold and coincidence triggering

- each polar column of detectors, overlapping with neighbors
- sum amplitude with conservative coincidence timing window
- compare to conservative energy threshold
- trigger when complementary (ECAL and HCAL) subsystems are both above threshold ~ only about 35 kHz

Electron subsystems

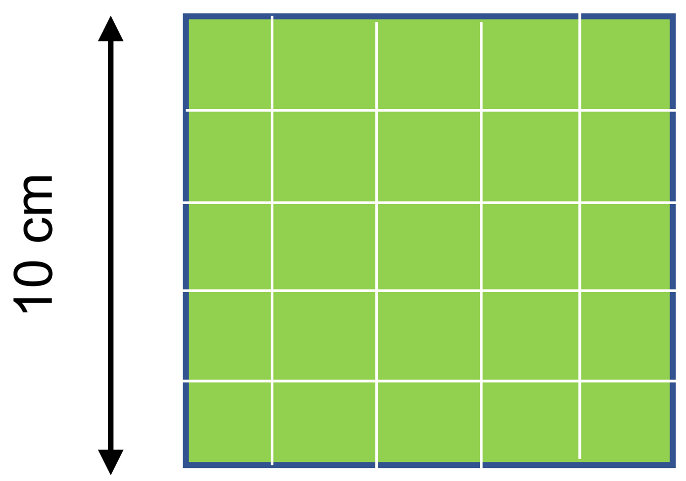

- 1200 $PbWO_4$ crystals
- 2x2x20 cm^3
- 5x5 grouping for subsystem
- 240 overlapping subsystems

Proton subsystems

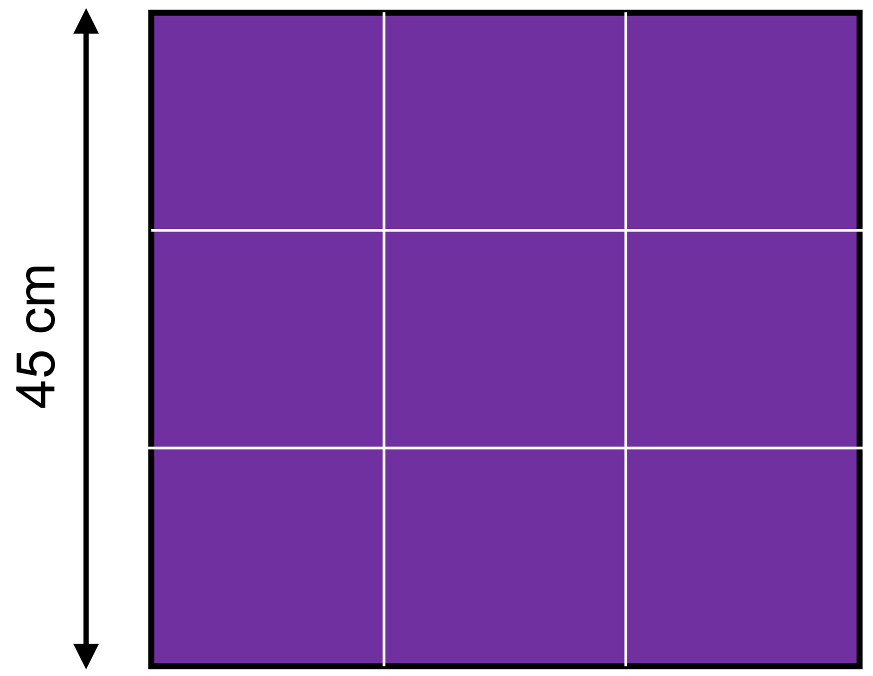

- 288 iron/scintillators
- 15.5x15.5x100 cm^3
- 3x3 grouping for subsystem
- 96 overlapping subsystems

Advantage: simplicity over dynamic clusterization, and fully sufficient for acceptance, resolution, and background

Fast Counting DAQ

250 MHz flash ADC (JLab **FADC250**) for HCAL and ECAL readout
Provides the pulse information for a fast, "deadtime-less" trigger

→

VTP (VXS Trigger Processor)
Running, updating sums over overlapping calorimeter clusters, to find ECAL+HCAL coincidence above threshold

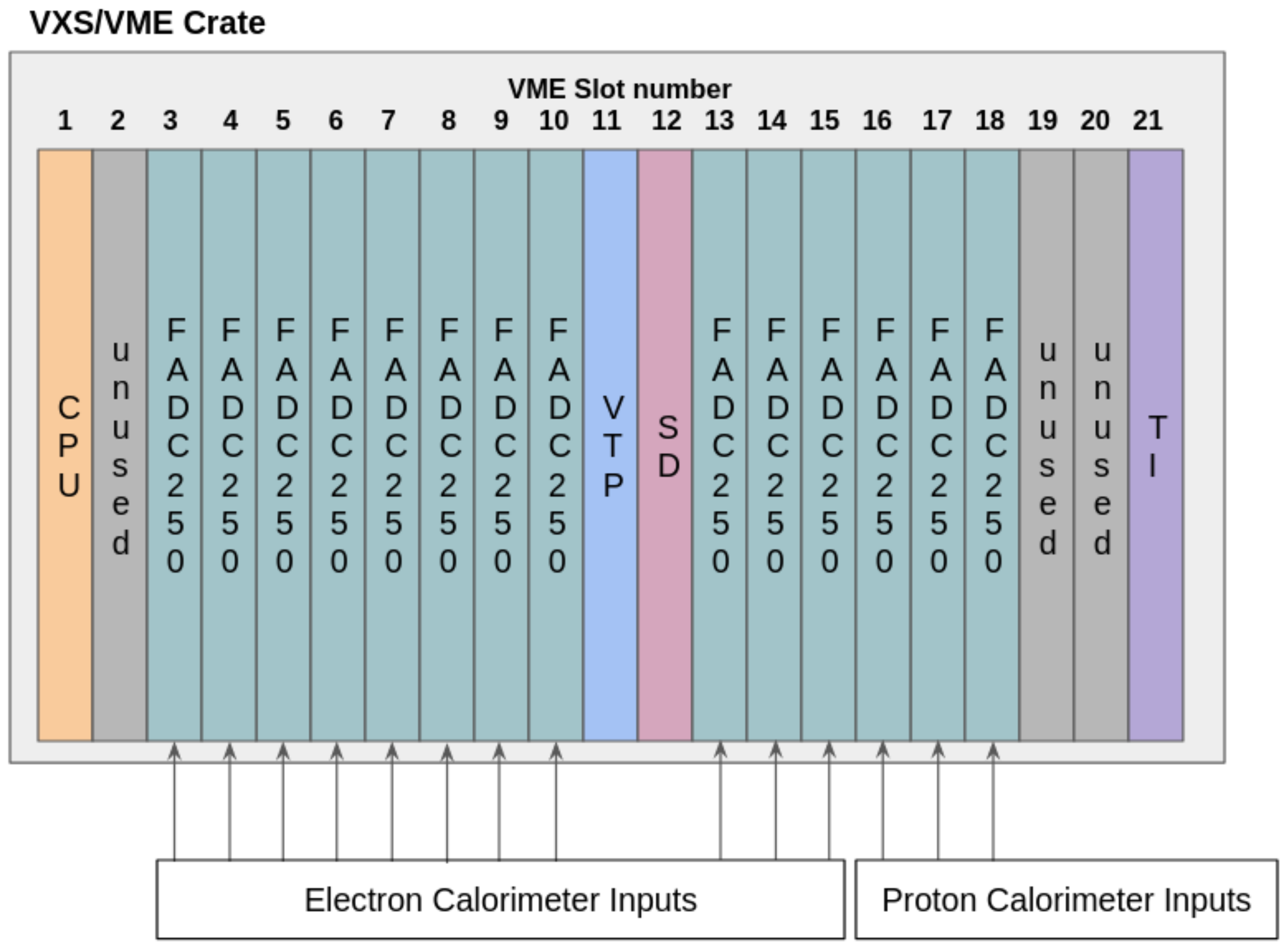

One VXS crate will handle one sixth of ECAL + HCAL,
also provide external trigger for ScintArray pipelineTDC readout

Corresponding scintillator elements recorded in TDC (pulse time, time over threshold) with each trigger

Expect ~35kHz total, ~500 Mb/s data rate,
distributed over 6 separate crates (calorimeters) and 3 crates for scintillators

JLab Fast Electronics FADC250 / VTP

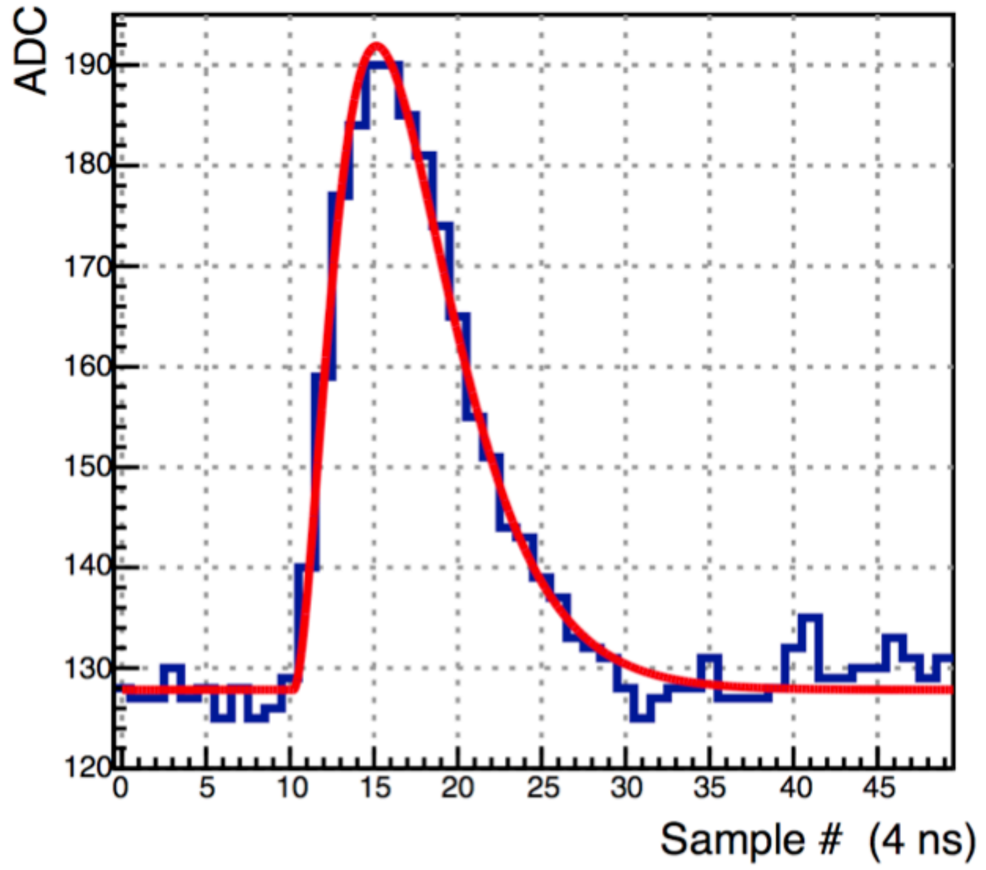

JLab FADC250 for HCAL and ECAL readout
Provides the input for a fast, "deadtime-less" trigger

FADC Trigger path: Pulse detector/integrator

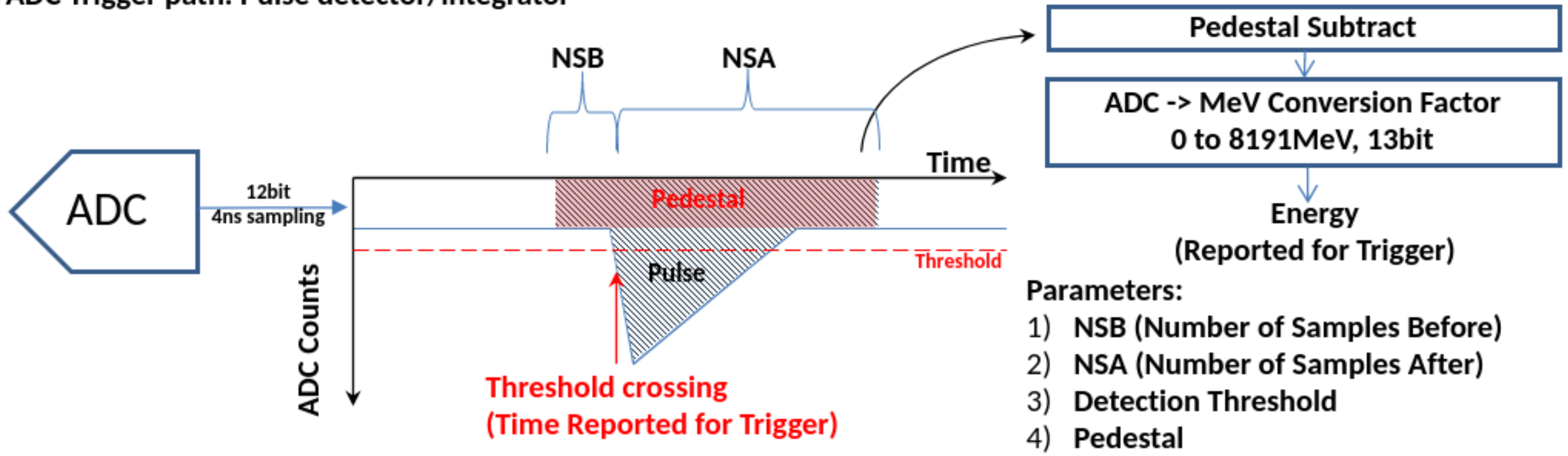

Parameters:

1) **NSB (Number of Samples Before)**
2) **NSA (Number of Samples After)**
3) **Detection Threshold**
4) **Pedestal**
5) **Gain**

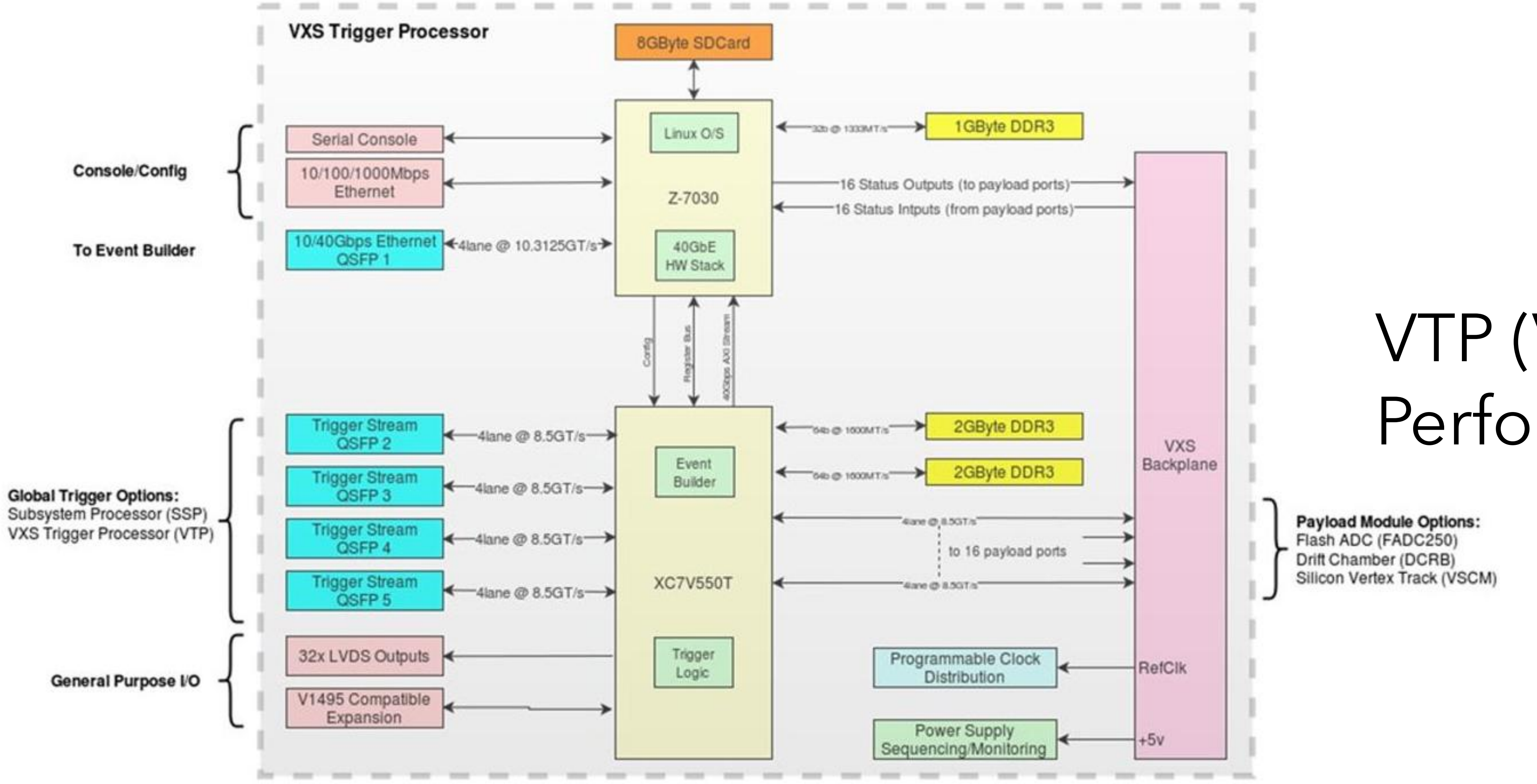

VTP (VXS Trigger Processor)
Performs the trigger logic computation

Scintillator TDC readout

Two workable options, based on previously implements MAPMT pipeline readout

model based on CDET detector (GEP)

- NINO chip module, **VETROC** for scintillator readout.
- Need 38 boards, 3 crates.
- Pipeline event record triggered by calorimeter coincidence trigger.
- Use HCAL subsystem number to select scint elements for readout
- Record time, time-over-threshold for scint elements **(preferred)**
- 35 kHz trigger rate, 8 Bt/read, 225 elements = 65 MB/sec

model based on CLAS12 RICH

- MAROC3a FPGA readout module
- discriminated signal
- SSP readout board for scintillator readout.
- Need 38 front-end boards, 2 SSP, 1 crate.
- Event record triggered by calorimeter coincidence trigger.
- All elements recorded hit or not, 35kHz*7200 bits = 32 MB/sec

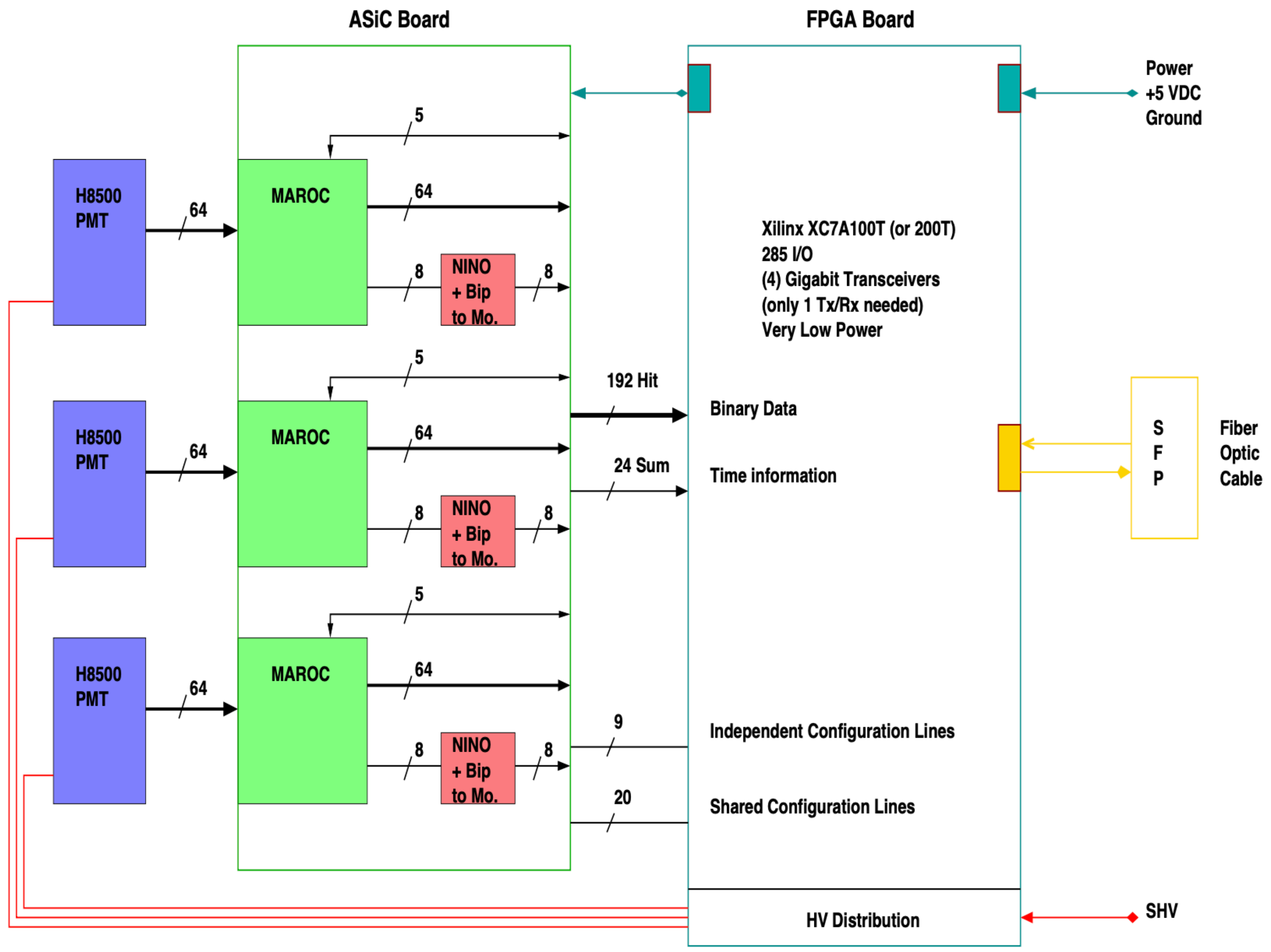

Other possible discriminator boards, if availability is limited (such as SAMPA…)

PV measurements are an established technique

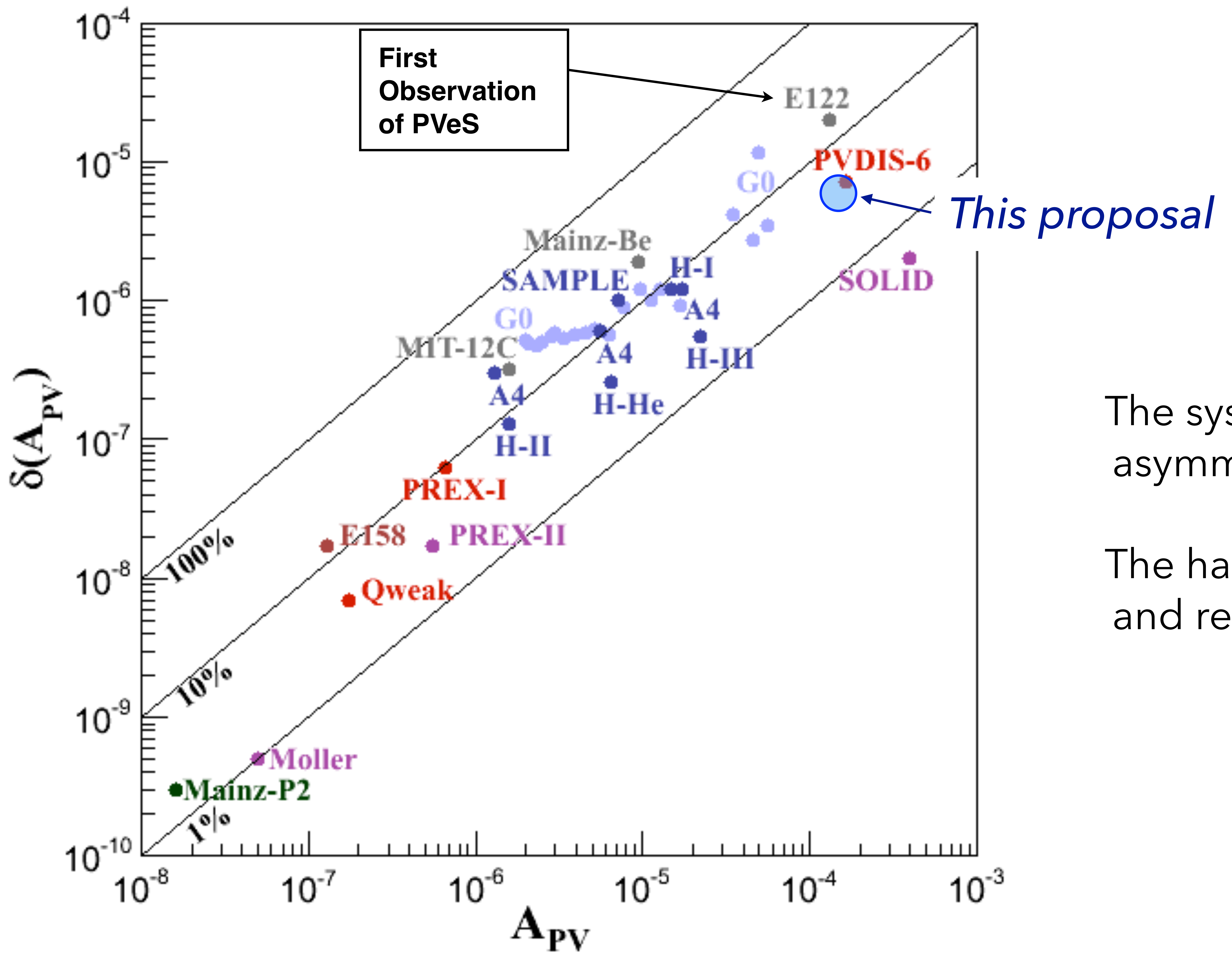

The systematic error of measuring a small asymmetry wouldn't really the hard part

The hard part is what is getting enough rate, and removing enough background